Geodesic Grids and Hybrid Vertical Coordinates

Acknowledgments

Ross Heikes

Celal Konor

The Platonic Solids

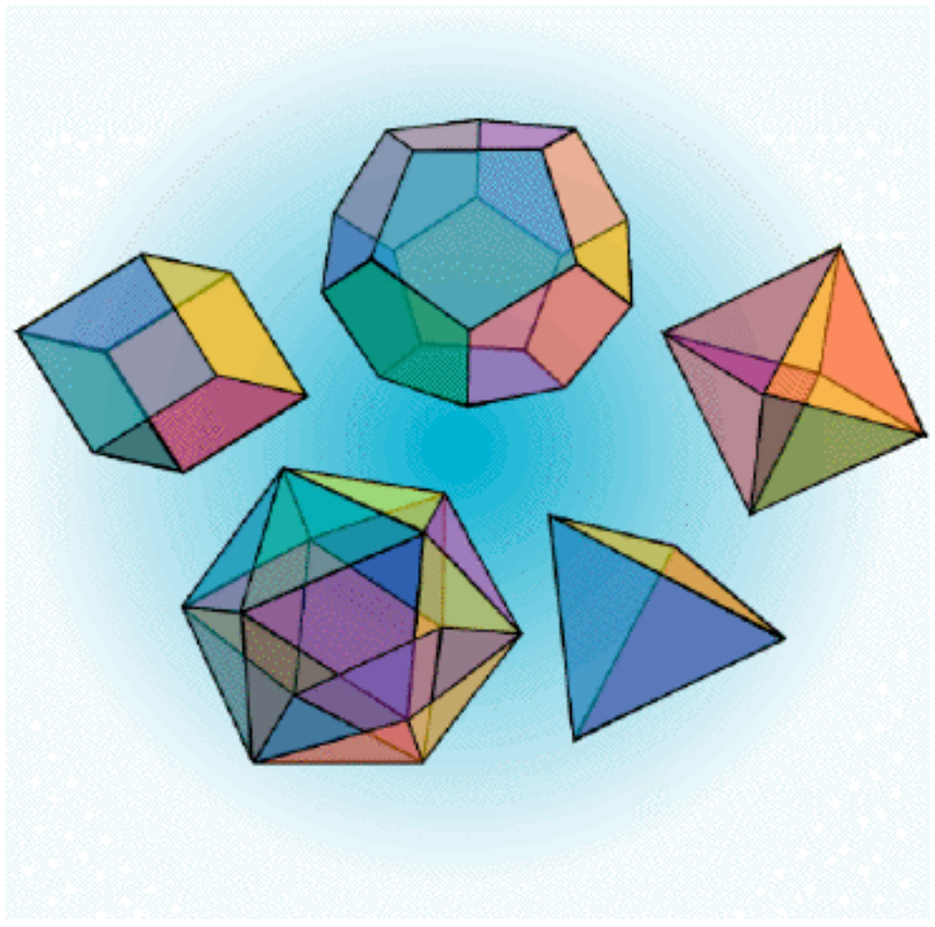

Geodesic Grid

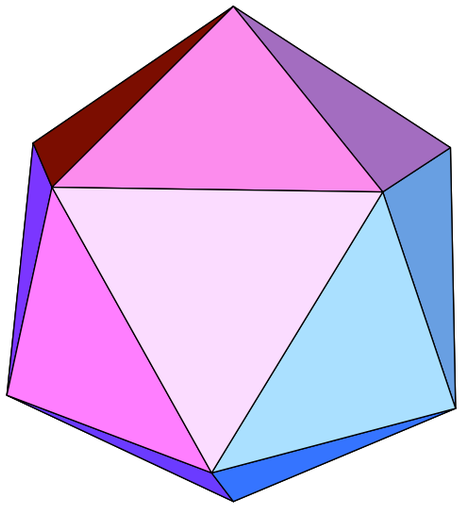

Icosahedron

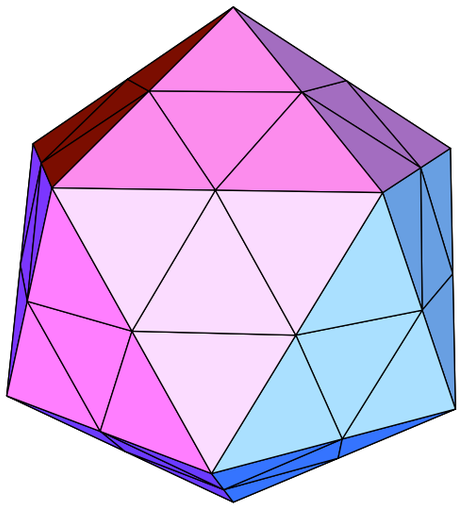

Bisect each edge and connect the dots

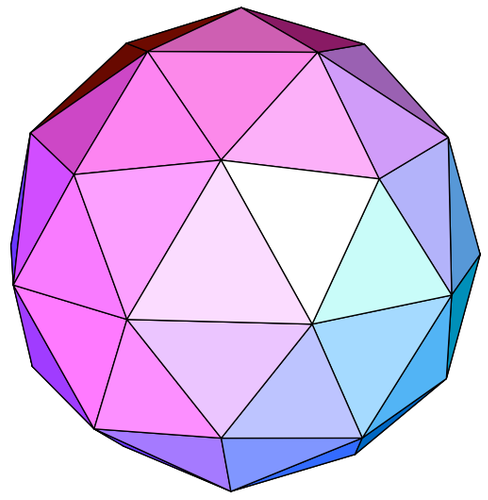

Pop out onto the unit sphere

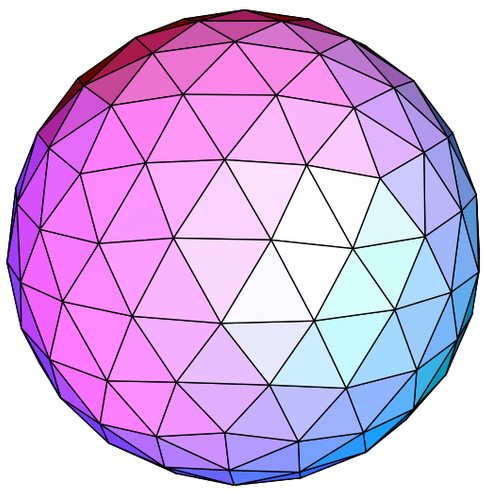

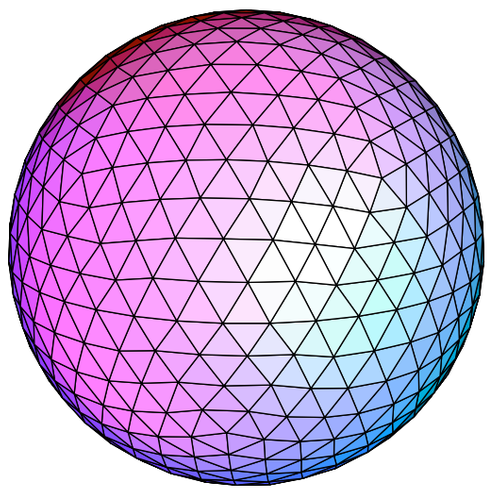

And so on, until we reach our target resolution...

Voronoi cells

An area is associated with each vertex. These " Voronoi cells" are the control volumes of the finite-difference operators.

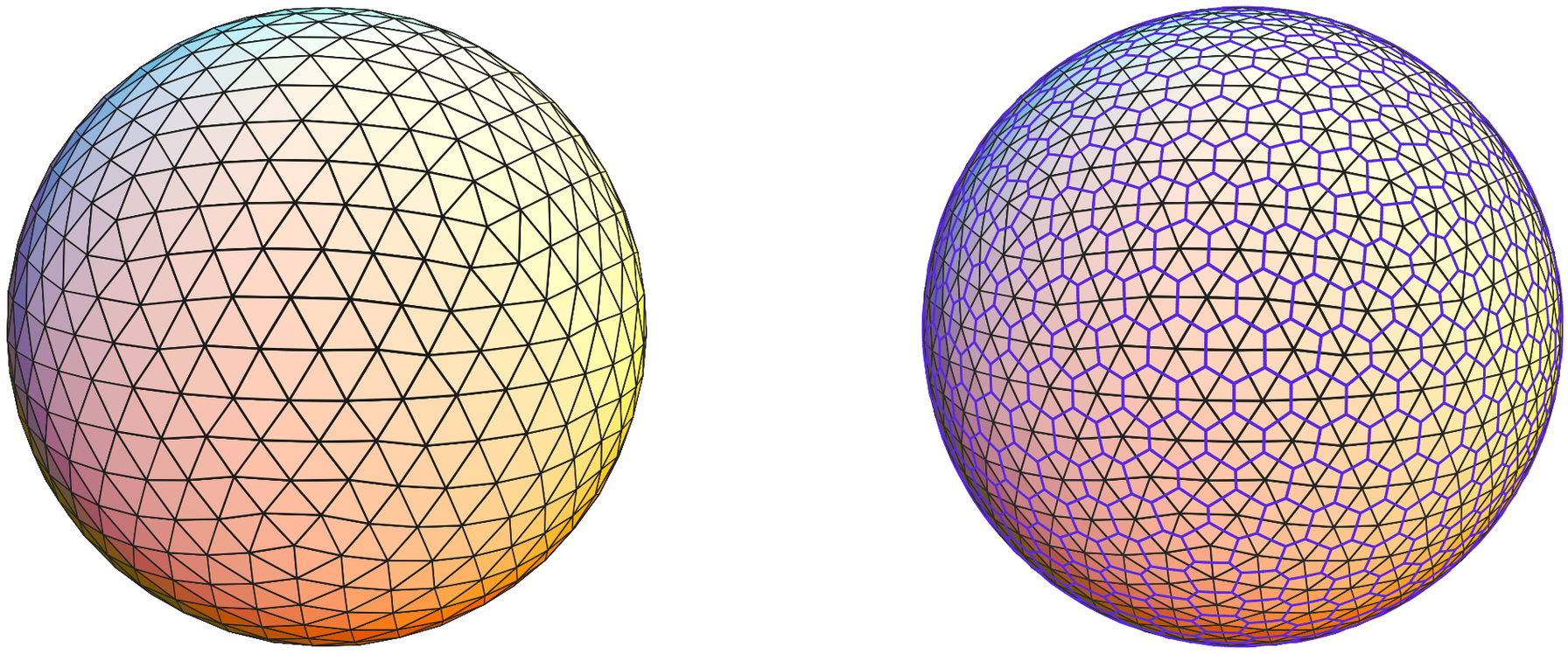

There are 12 pentagons (associated with the vertices of the original icosahedron) and N-12 hexagonal cells.

This grid eliminates the pole problem and provides approximately *homogeneous* and *isotropic* resolution over the sphere.

Counting the cells

The global number of grid points is given by

$$N = 2 + 10 \times 2^{2r}$$

where r is number of applications of the subdivision algorithm.

Lat-Lon Versus Geodesic Grids

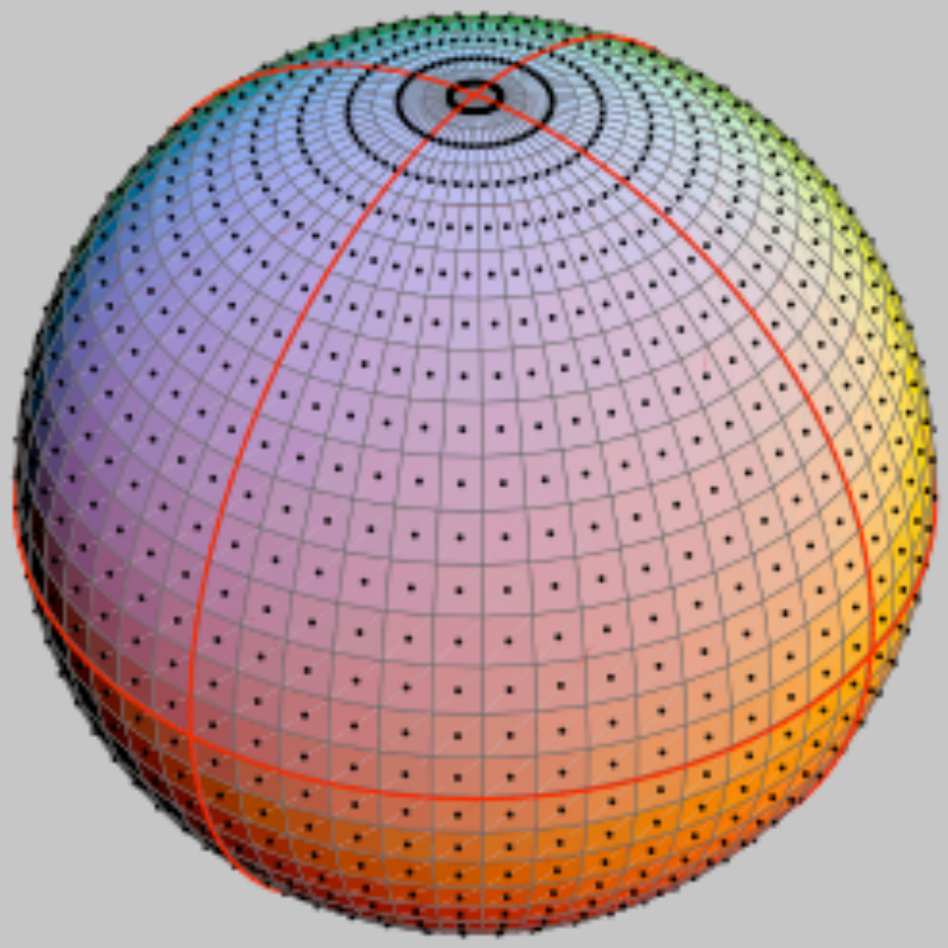

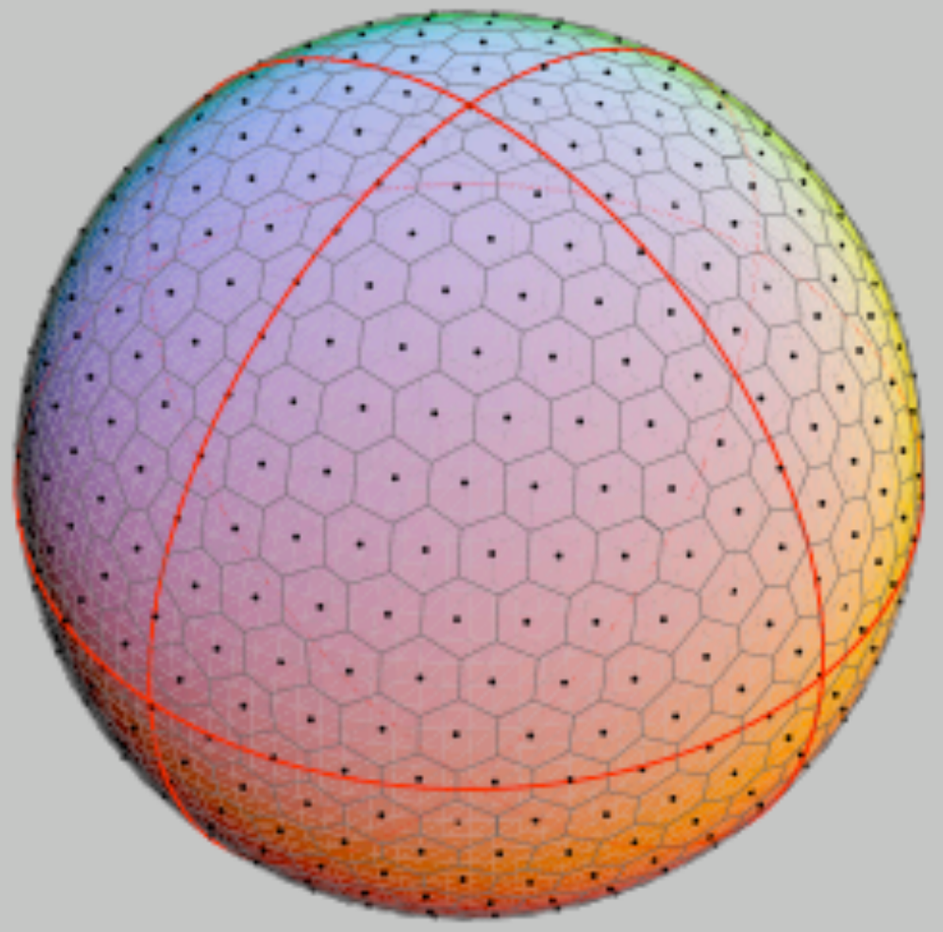

Variationally “tweaked” geodesic grids

Recursion number	Number of cells	Average distance between cell centers, km	Area ratio (smallest to largest)
0	12	7054	1
1	42	3717	0.885
2	162	1909	0.916
3	642	961	0.942
4	2562	481	0.948
5	10242	240	0.951
6	40962	120	0.952

Tiling the Plane

12 neighbors
3 wall neighbors

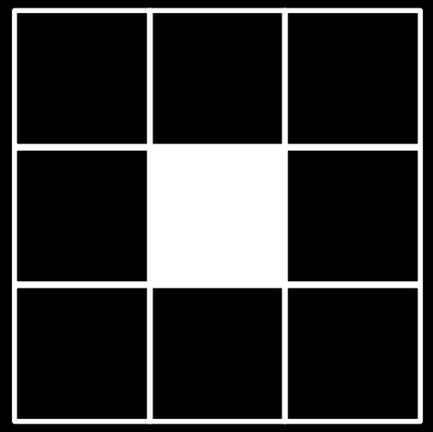

8 neighbors
4 wall neighbors

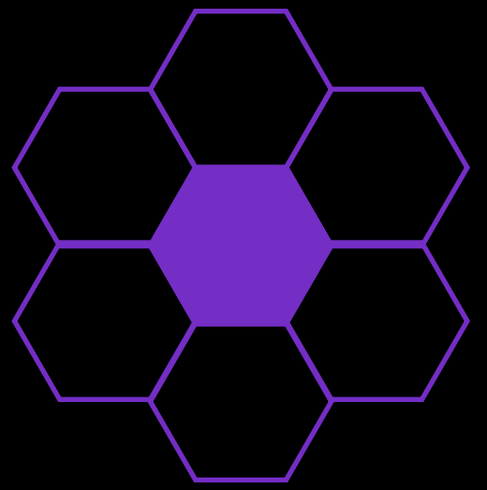

6 neighbors
6 wall neighbors

Triangles
nest.

Squares
nest.

Hexagons
don't nest.

Springs

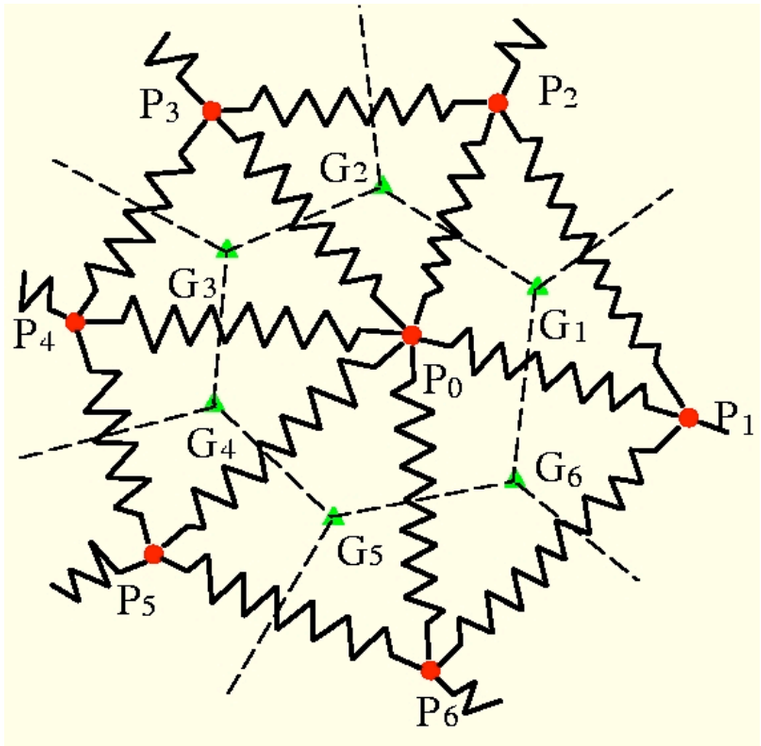

Following Tomita et al. (2001), "springs" can be used to vary the grid spacing over the sphere.

Finite-differences on geodesic grids

Example: For a scheme of the form

$$(\nabla^2 f)_j \cong \sum_{k'=-\infty}^{\infty} e_{j,k'} f(\lambda_{j,k'}, \varphi_{j,k'})$$

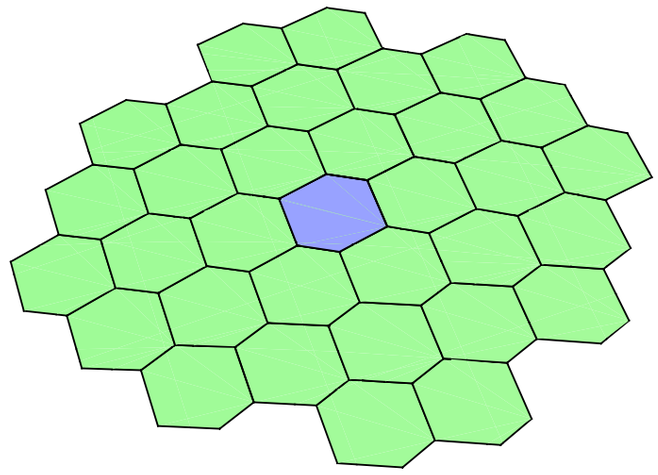

$$f(\lambda_{j,k'}, \varphi_{j,k'}) = f(\lambda_j, \varphi_j) + [\delta\lambda_{j,k'} f_\lambda + \delta\varphi_{j,k'} f_\varphi] +$$

$$\frac{1}{2!}[\delta\lambda_{j,k'}{}^2 f_{\lambda\lambda} + 2\delta\lambda_{j,k'}\delta\varphi_{j,k'} f_{\lambda\varphi} + \delta\varphi_{j,k'}{}^2 f_{\varphi\varphi}] + \ldots$$

we must satisfy

$$\sum_{k'=-\infty}^{\infty} e_{j,k'} = 0$$

and nine more linear equations to get second-order accuracy.

And so on...

To get higher accuracy, we must satisfy more equations.

To satisfy more equations, we need more "unknowns."

To get more unknowns, we must use a larger stencil.

The whole procedure can be automated by writing a computer program, e.g., using software like *Mathematica*.

This is standard material.

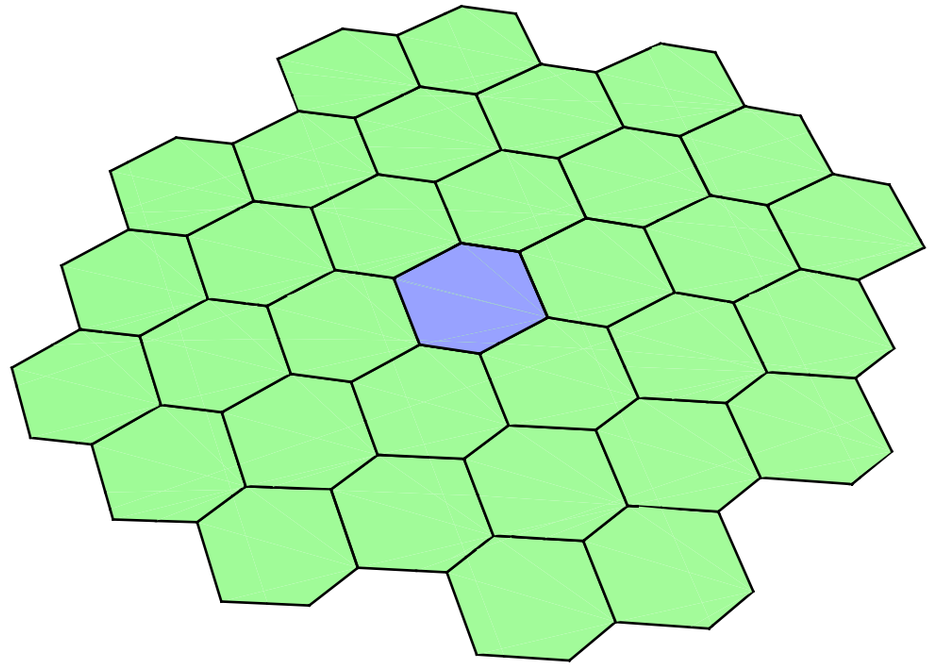

Laying it out

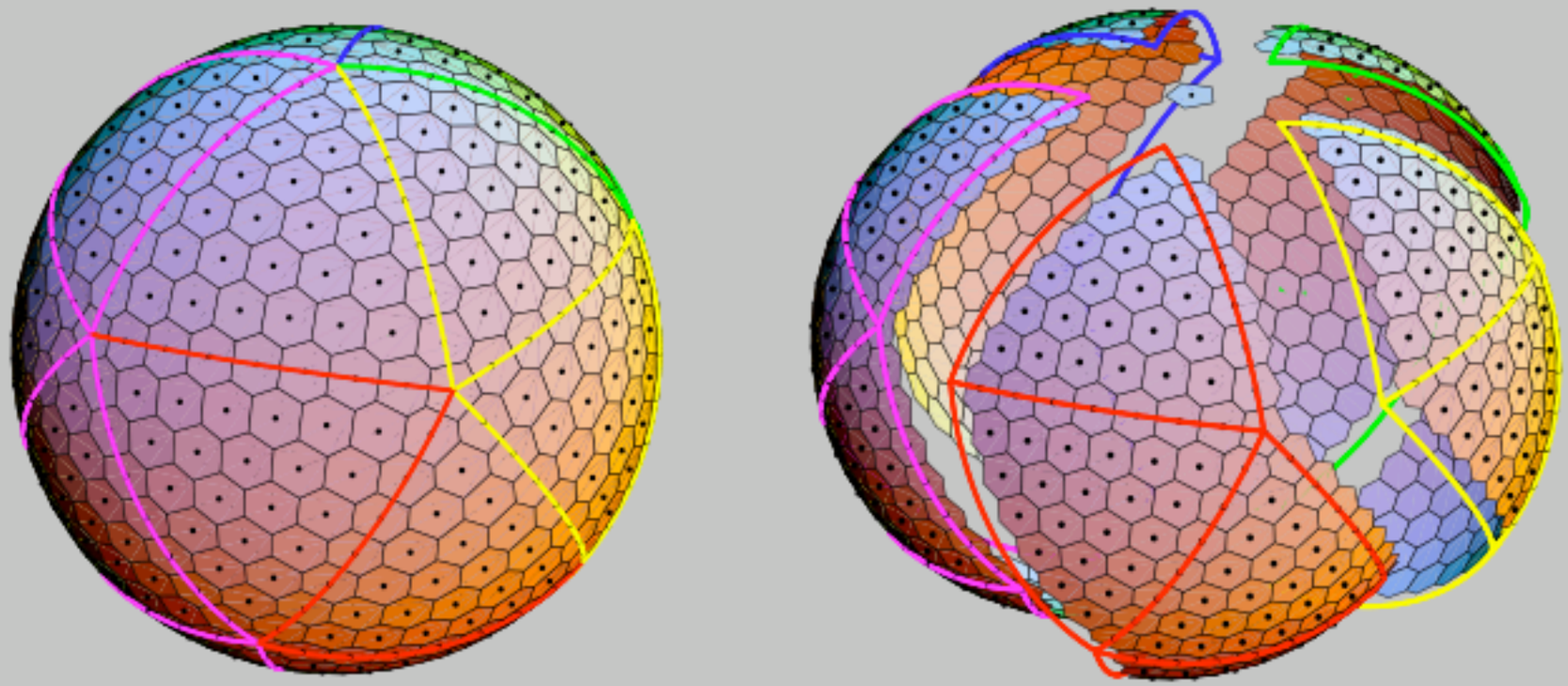

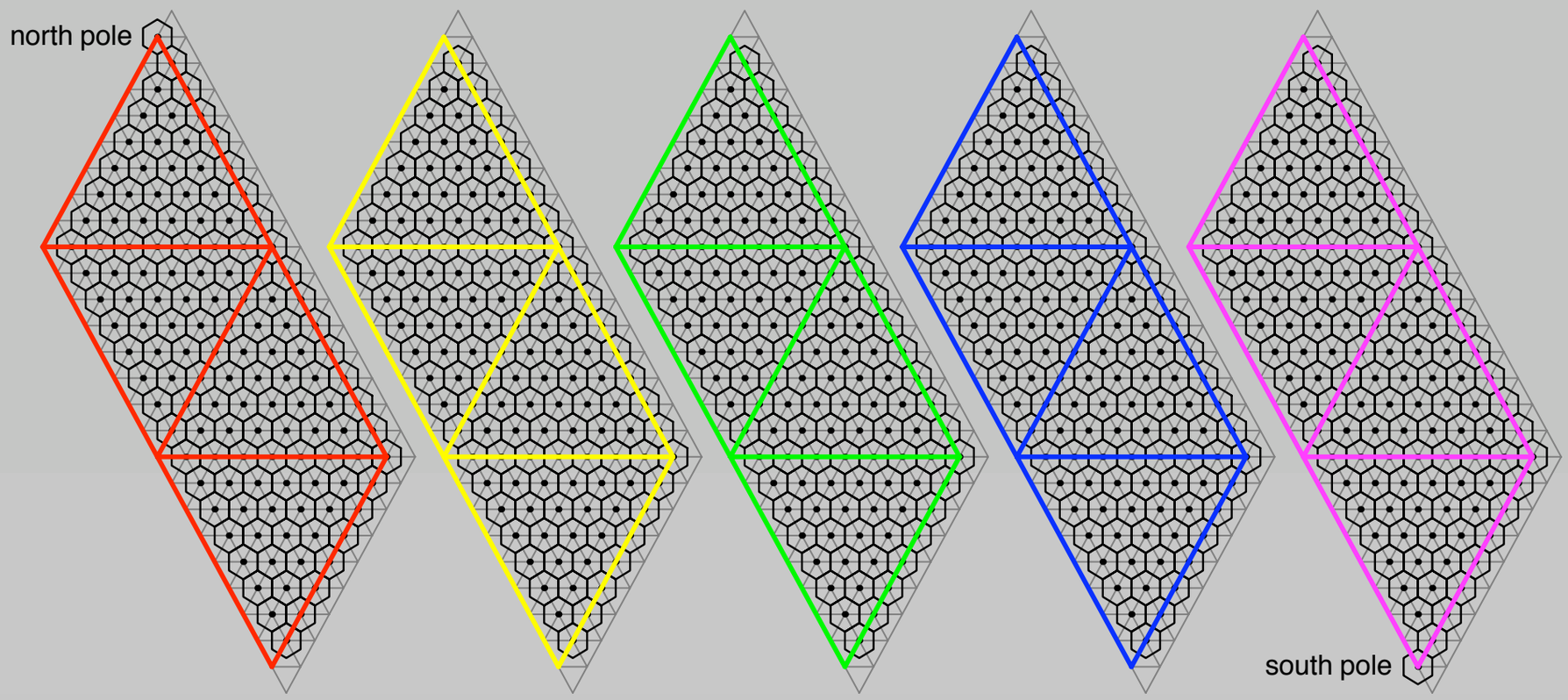

Parallel domain decomposition

Concatenating the faces of the icosahedron allows the sphere to be partitioned into 10 quadrilateral subdomains.

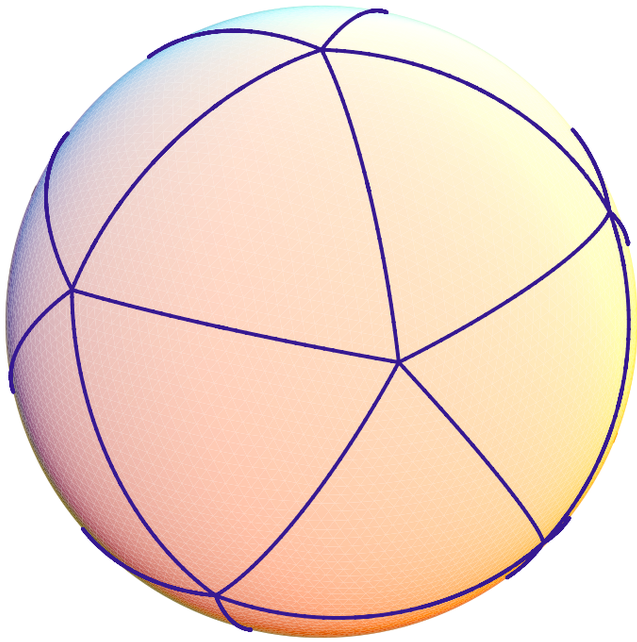

Icosahedron projected to sphere

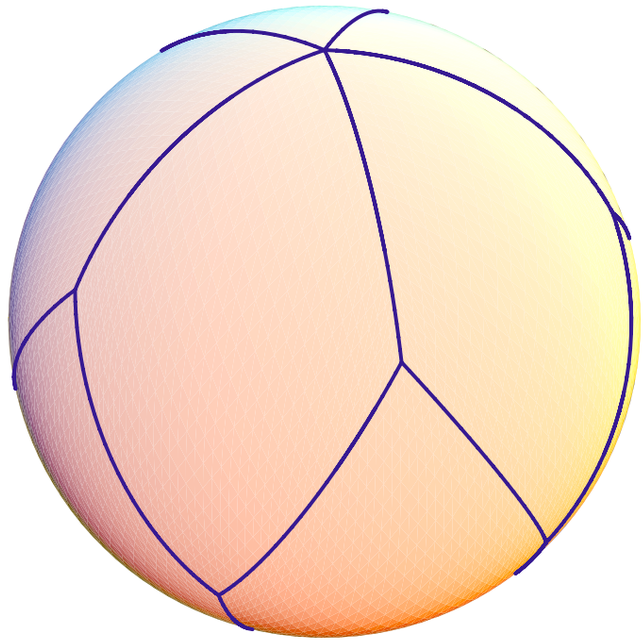

10 quadrilateral regions

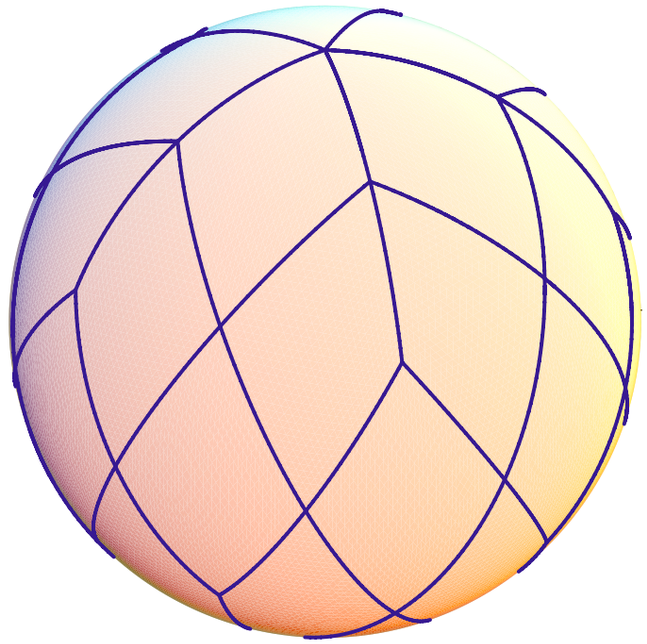

40 quadrilateral regions

The cells within a given subdomain are assigned to a process.

Any subset of the global number of subdomain can be assigned to a process. However, to maintain load balance, the number of processes must evenly divide the number of subdomains.

Two-dimensional data decomposition

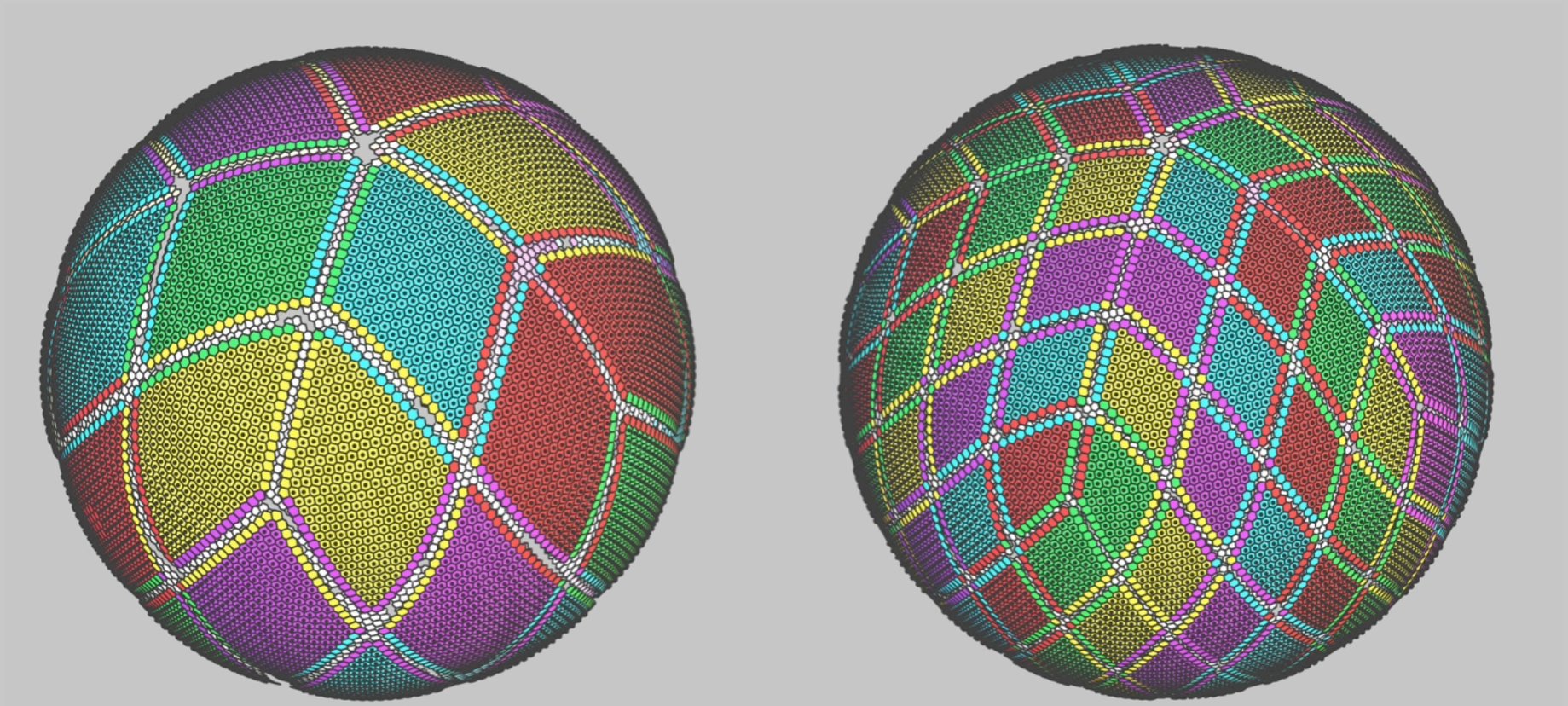

Each color corresponds to a processor. In this simplified example there are only four processors.

Trees are the answer.

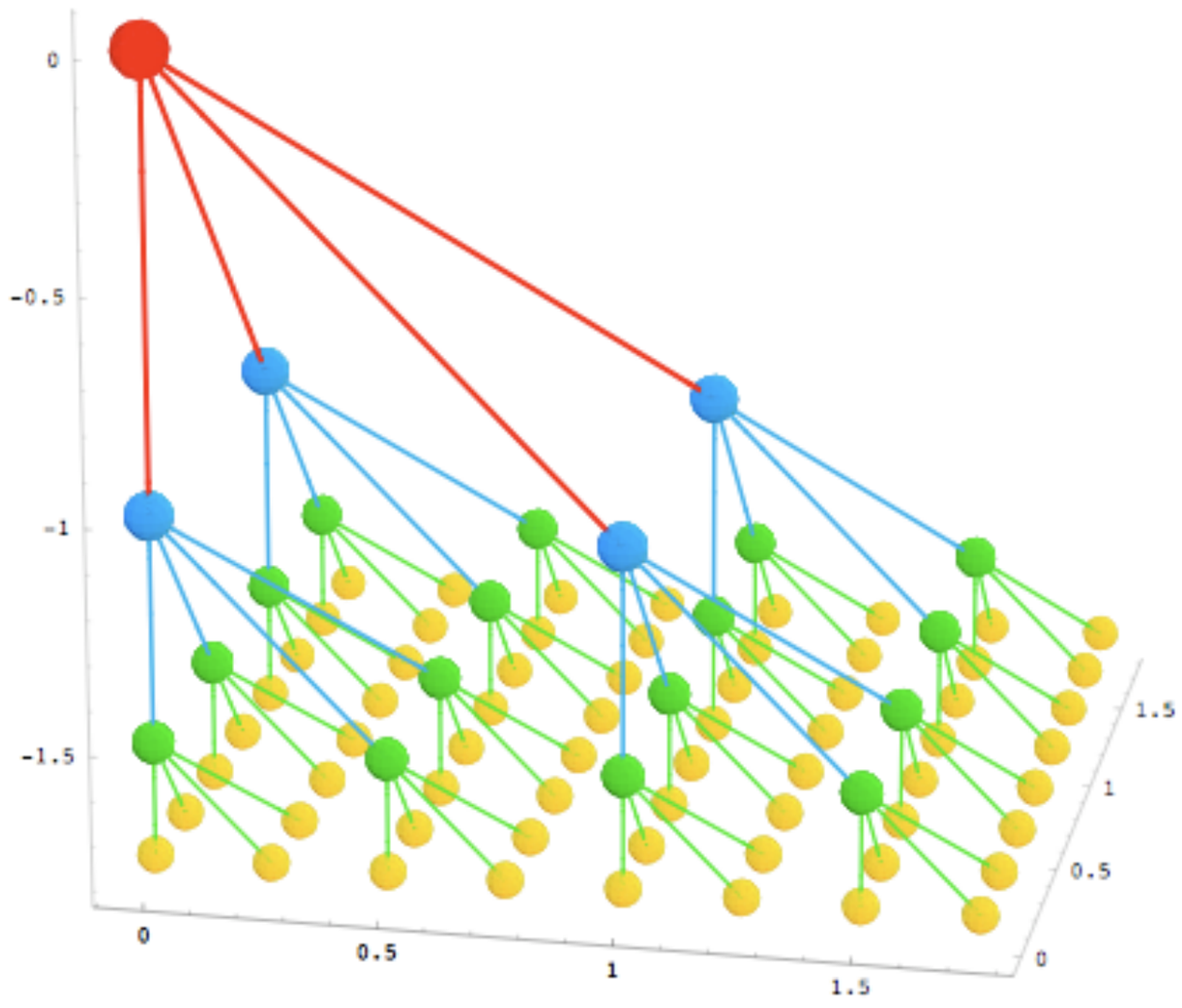

An alternative one-dimensional indexing scheme can be based on a tree-structure.

Not a “radical” idea

Williamson, and Sadourny et al., in the 60s

Baumgardner in the 80s,
leading in the late 90s to the operational DWD model

And now...

Our team (icosahedral since about 1994),
DWD,
Frontier Project,
MPI,
ESRL,
Peltier,
Thuburn

The Z-Grid

$$\frac{\partial \zeta}{\partial t} = -f\delta$$

$$\frac{\partial \delta}{\partial t} = f\zeta + g\nabla^2 h$$

$$\frac{\partial h}{\partial t} = -H\delta$$

$$\zeta = \nabla^2 \psi$$

$$\delta = \nabla^2 \chi$$

$$\mathbf{V} = \nabla\chi + \mathbf{k} \times \nabla\psi$$

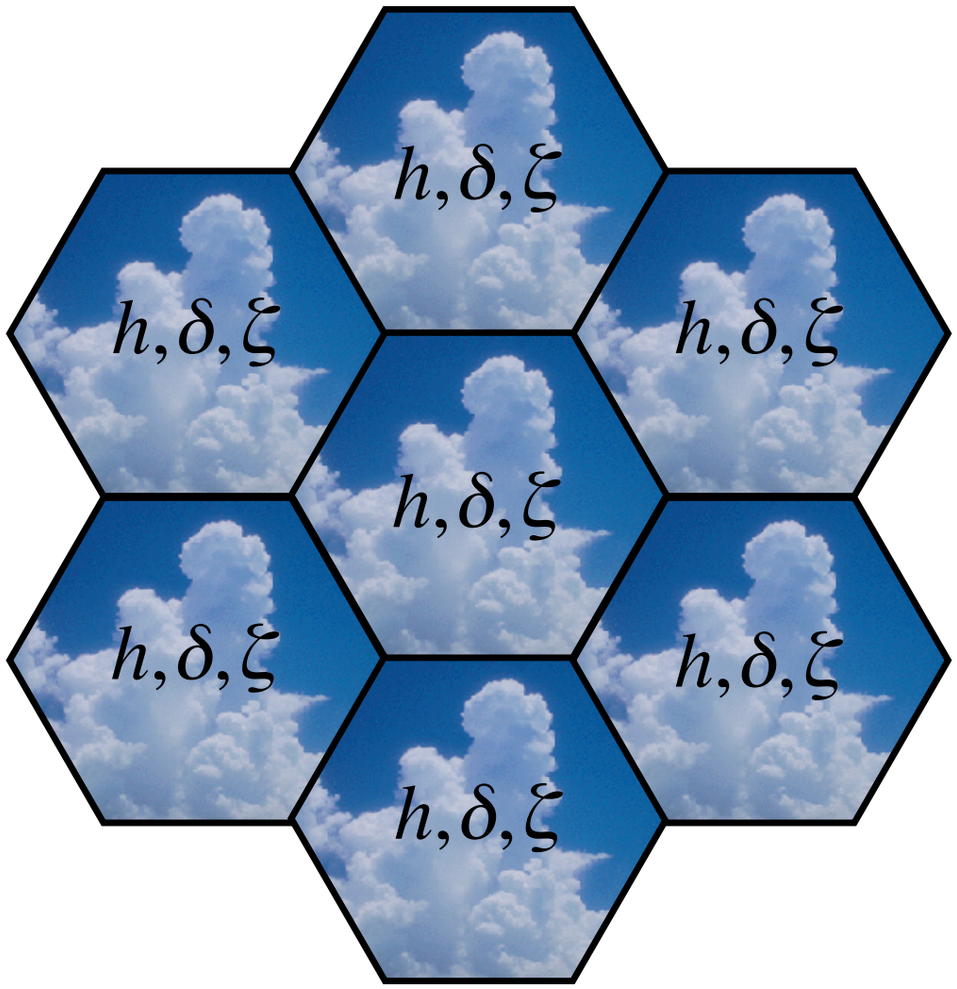

We use a multigrid method to solve the elliptic equations. It consumes about 15% of the dynamical core's run time.

Why use the Z-grid?

- **It gives a good simulation of geostrophic adjustment regardless of the ratio of the grid size to the radius of deformation (*Randall, MWR, 1994*).**

- **It has no computational modes.**

- **The concept is equally applicable to triangular, square, and hexagonal grids.**

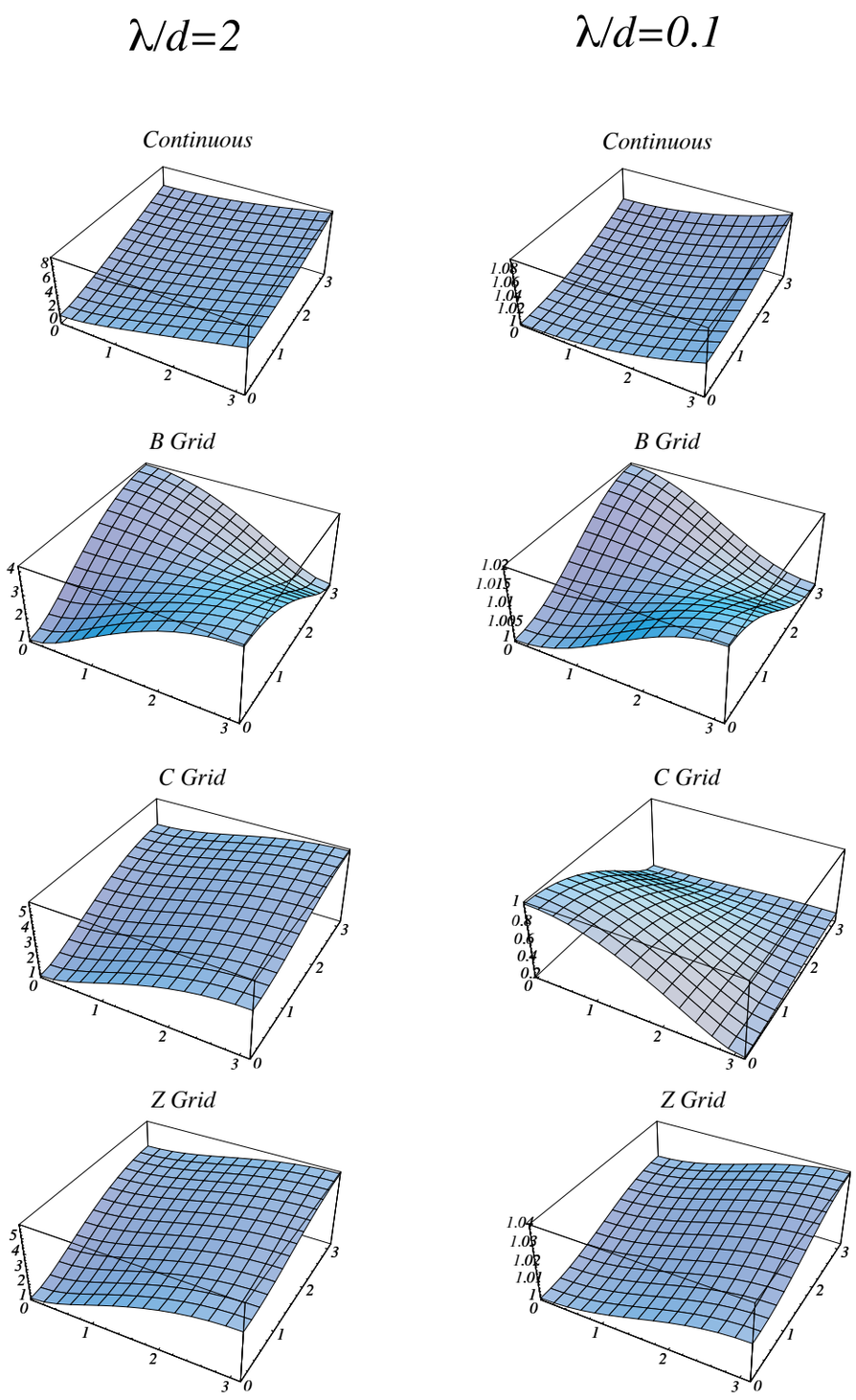

3rd-generation horizontal differencing

- The 2nd-order accurate fluxes of mass and tracers have been replaced with a more accurate 3rd-order scheme.
- The tracer equation reduces to the continuity equation when the tracer is spatially uniform.
- As an option, a flux-corrected transport algorithm combines these third-order fluxes with the first-order (upstream) fluxes to arrange the following:
  - For mass, sign-preservation.
  - For tracers, monotonicity.

First test the scheme in a 2D shallow-water framework with a modified version of Williamson test case one.

Advect a 1000 m high cosine bell around the sphere in 12 days with prescribed winds along a great circle.

Select the path to maximize encounters with pentagons.

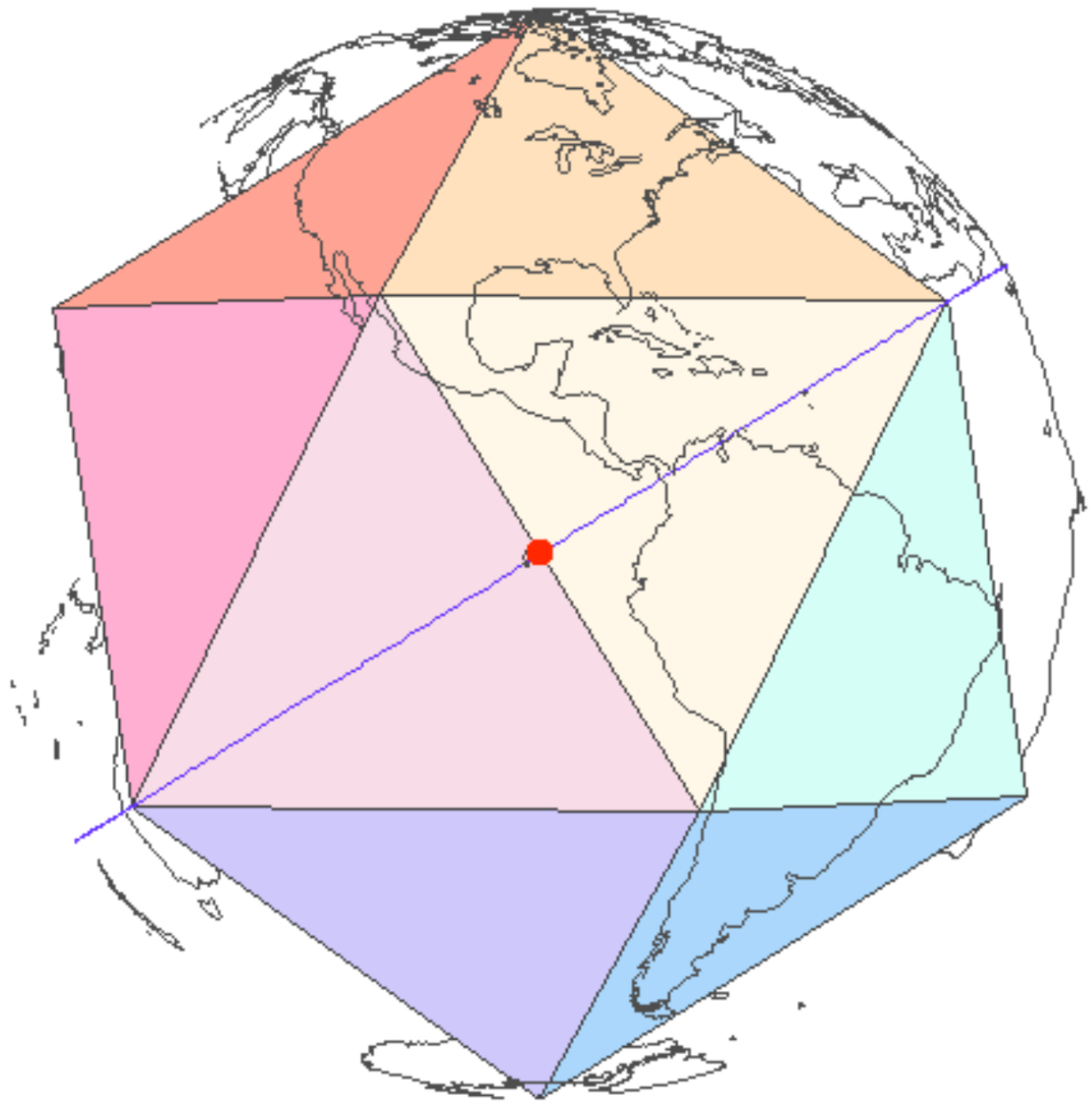

Cosine bell mass

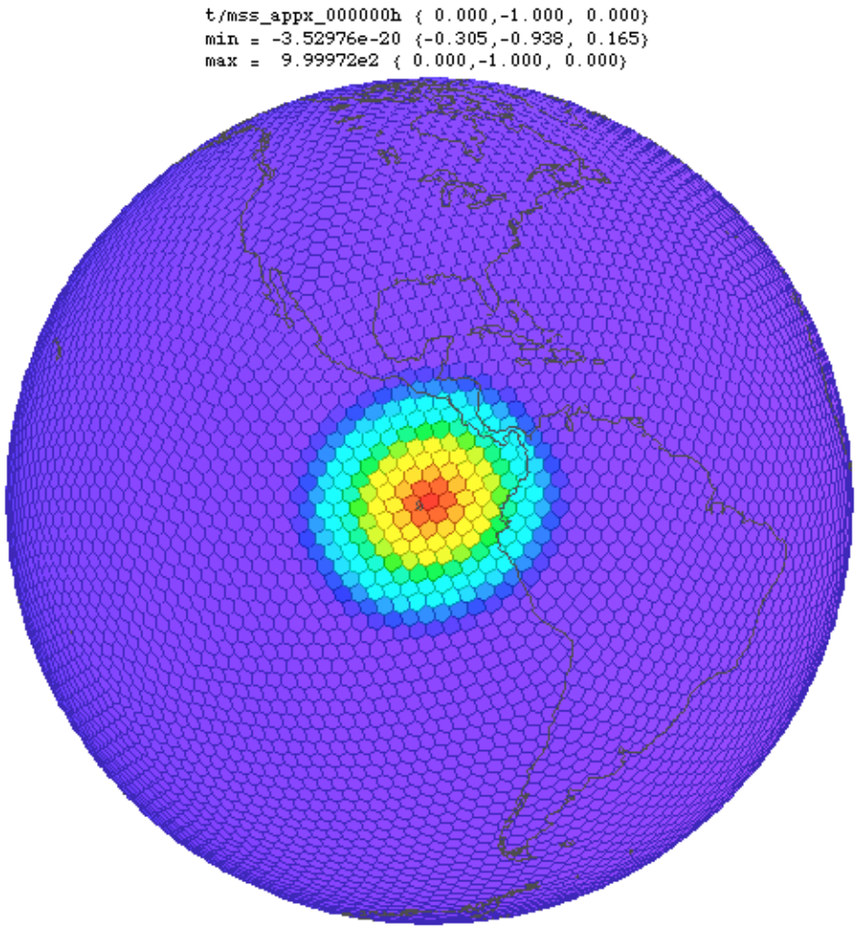

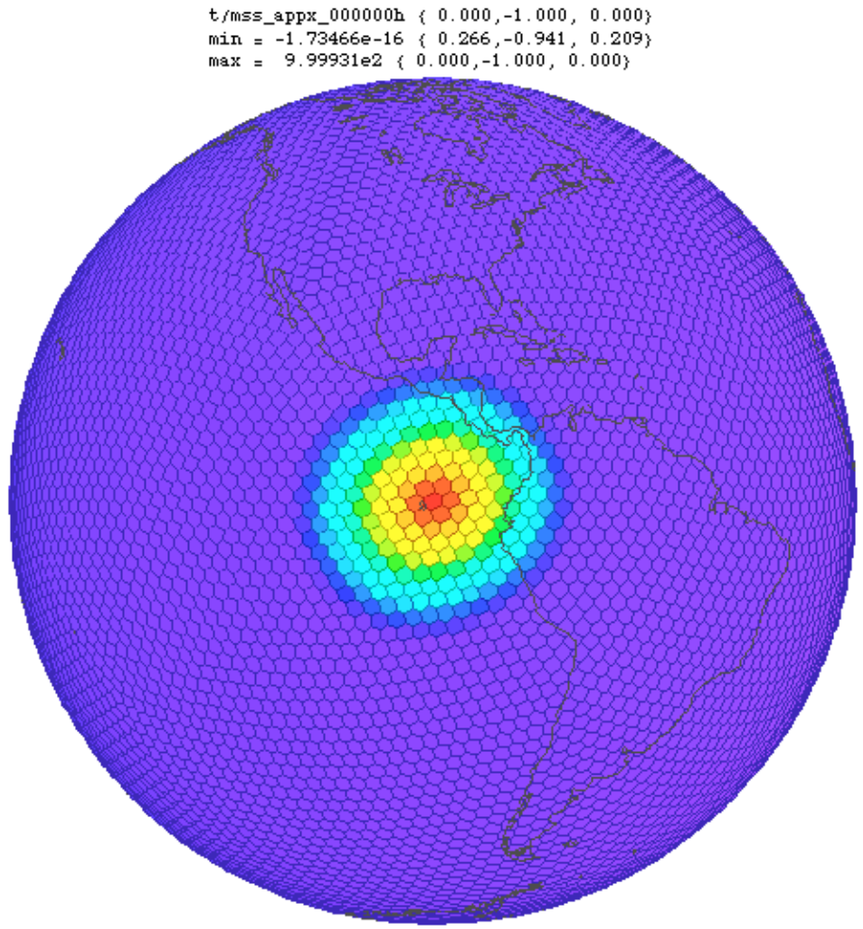

2nd-order

3nd-order

Both with FCT

Error norms with 10242 cells

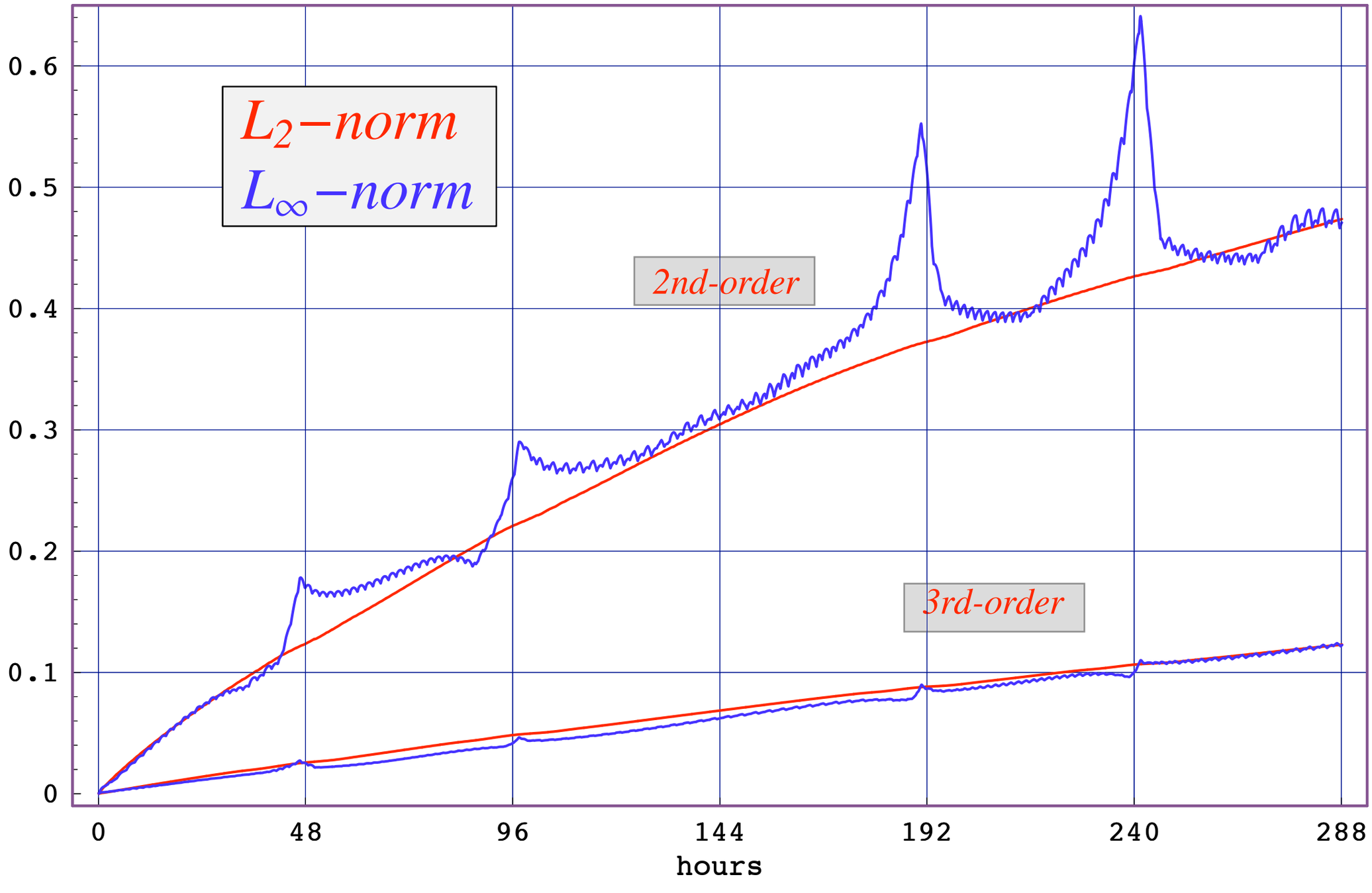

Initial Condition for 2D Surface-Wave Simulation
Hexagonal Model

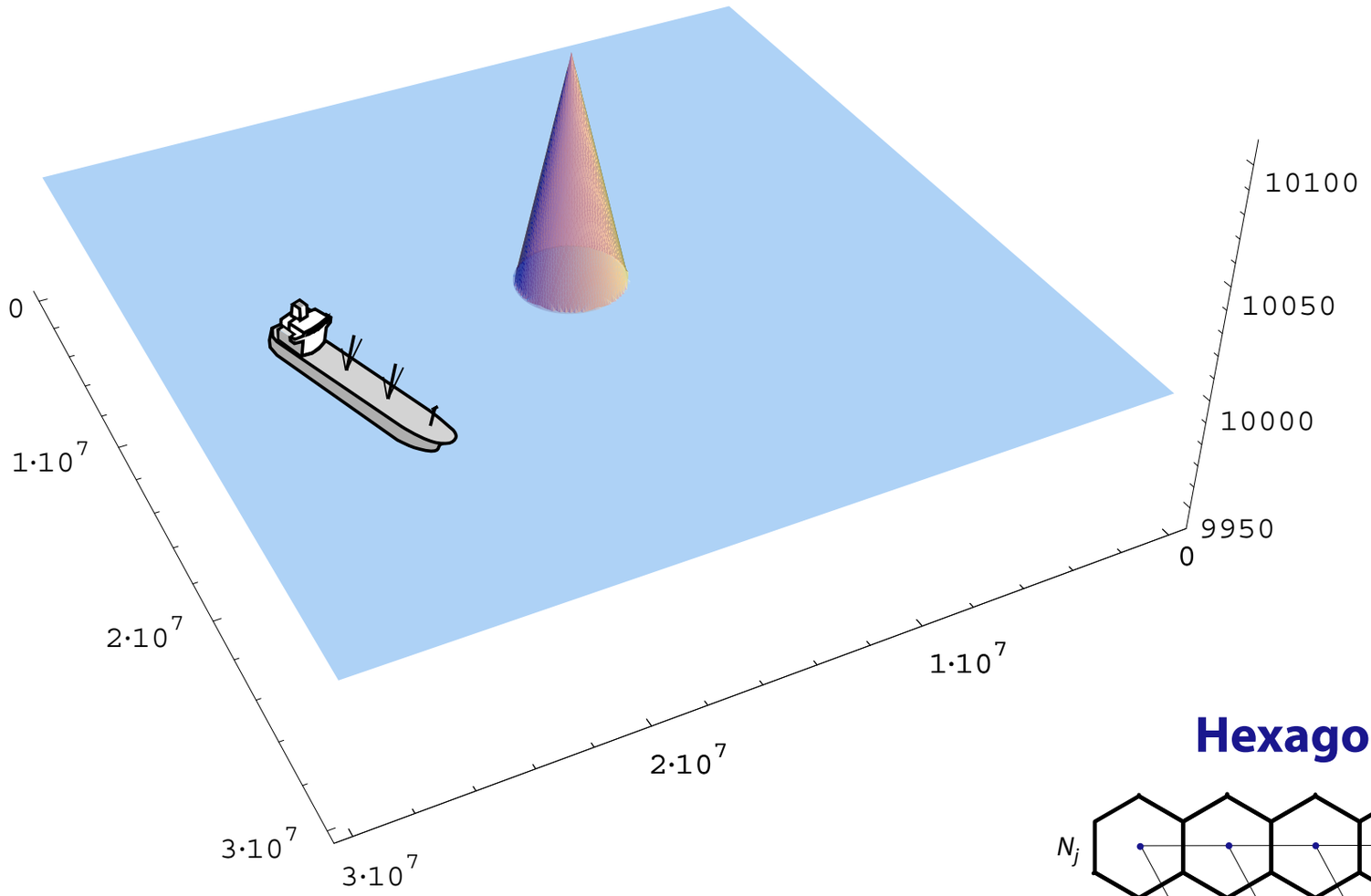

- h = 10000 m and h'_{max}=100 m
- (2ℓ)=100 km
- *Cyclic boundary conditions*

Hexagonal grid

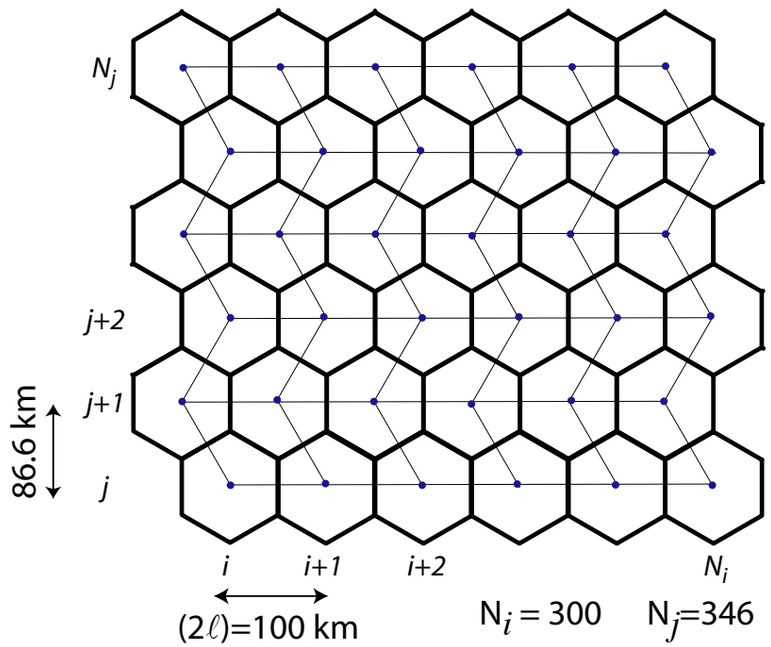

Hexagonal grid

Δt = 27 mins
“μ=5”

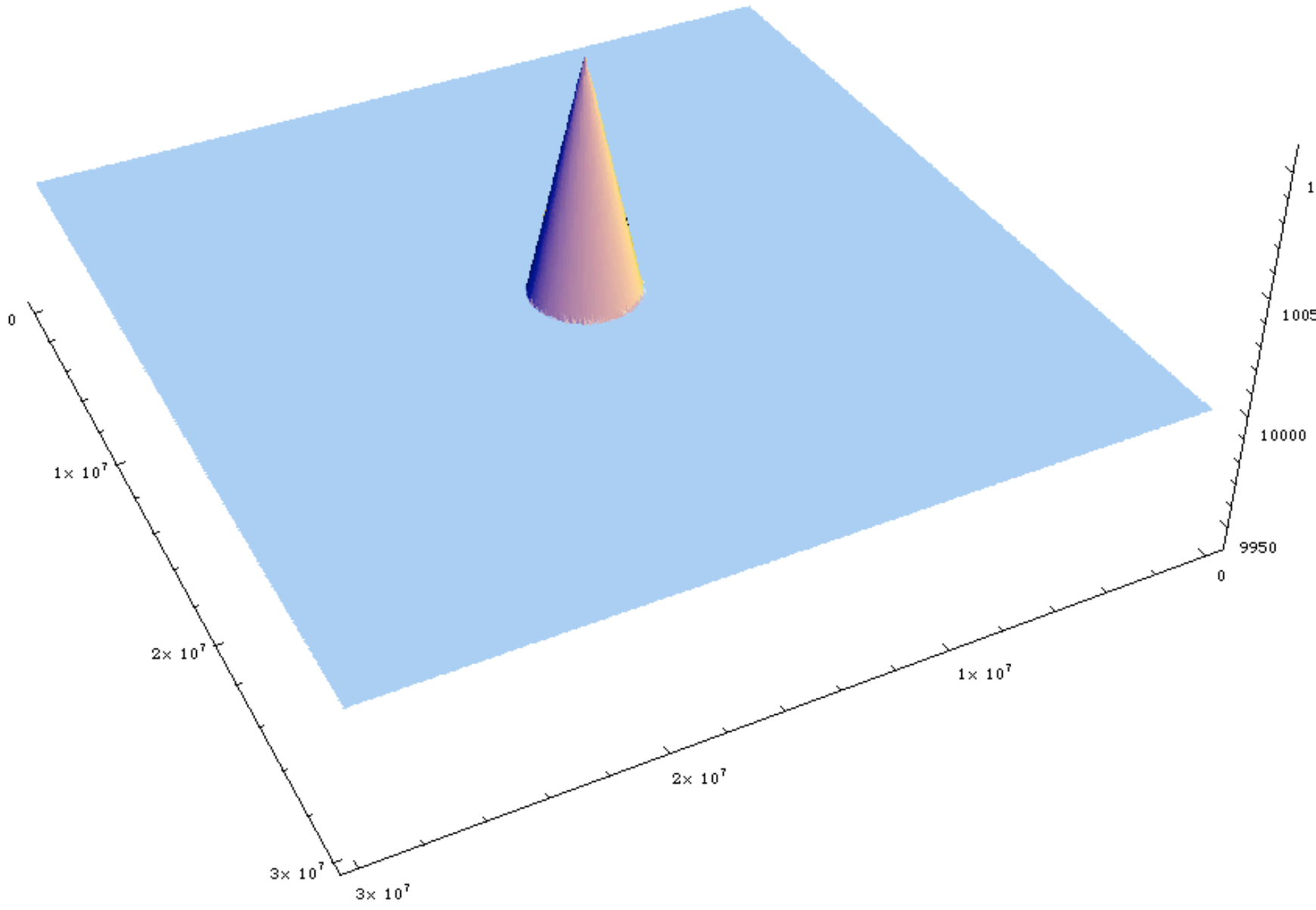

Advocates of theta coordinates

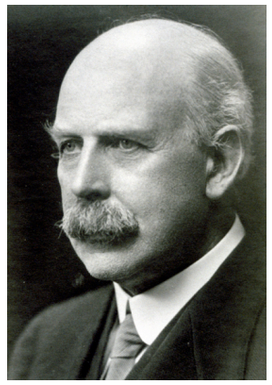

Napier-Shaw

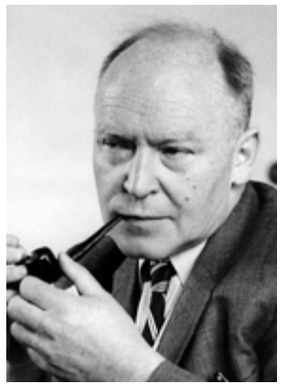

Rossby

Danielsen

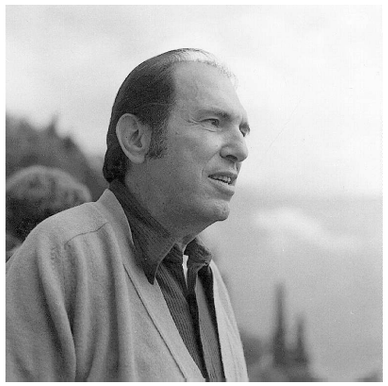

Namias

Starr

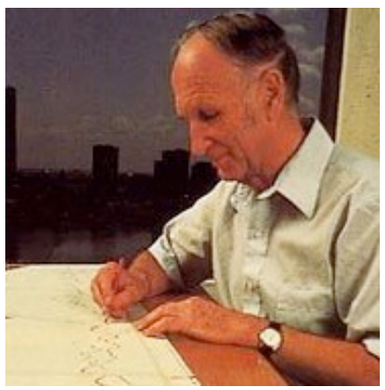

Lorenz

Eliassen

Johnson

Bleck

Benjamin

Hoskins

Arakawa

The lure of theta coordinates

- There is no "vertical motion" in the absence of heating.
  - This minimizes errors associate with vertical advection.
- The pressure-gradient force is a gradient.
  - This minimizes pressure-gradient errors near topography, and spurious generation of vorticity.
- The potential vorticity is easily accessible from the wind vector.
- Wave momentum transport occurs via isentropic form drag.
- It is easy to implement diffusion along theta surfaces.
- Both energy and entropy can be conserved (ref Don Johnson).
  - Relevant to the "cold pole" problem?
- An embedded PBL becomes more attractive.

But theta surfaces intersect the ground.

Theta coordinates

Where the theta coordinate intersects the Earth's surface, we can define "massless layers," following Lorenz (1955).

Sign-preserving advection schemes such as FCT can be used to deal with massless layers.

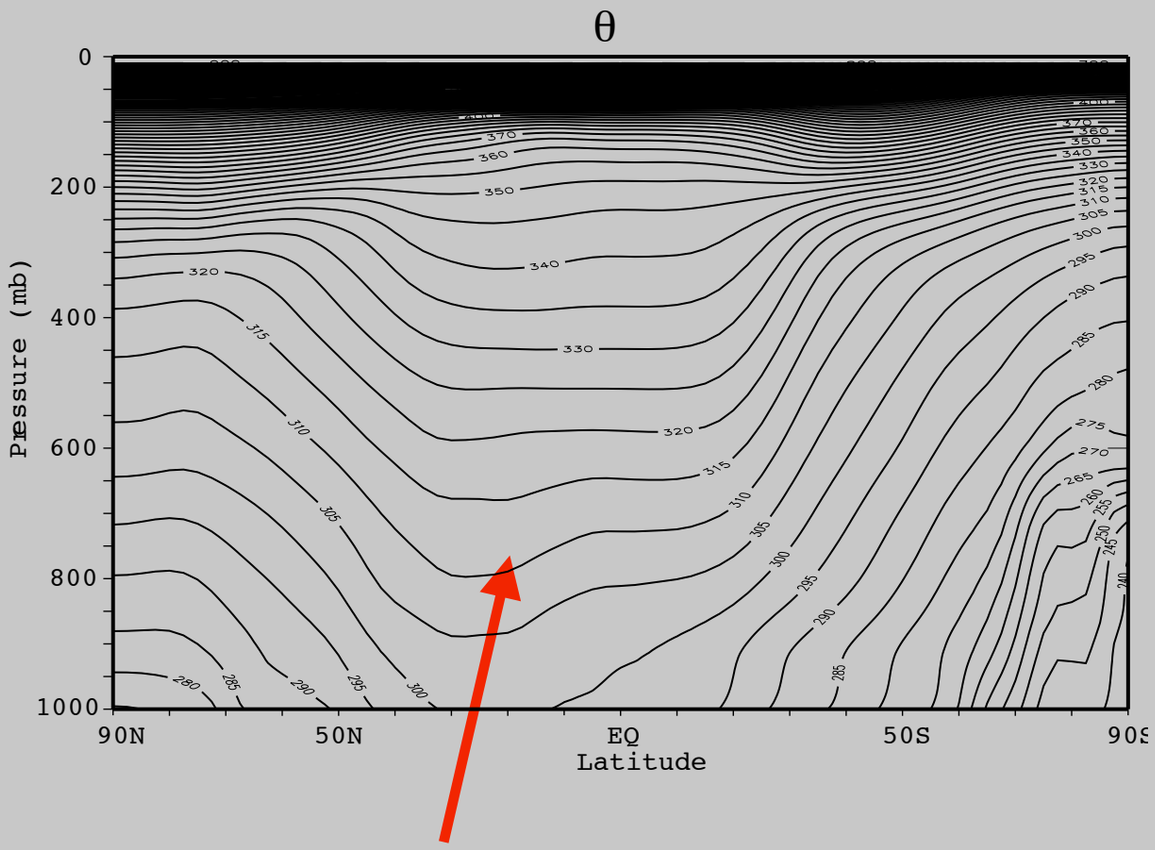

Note spreading of isentropes in the tropical troposphere. Many theta layers are "wasted" in the tropics.

In order to have adequate vertical resolution over the entire globe, it is necessary to allocate many theta layers. A hybrid sigma-theta coordinate helps with this problem.

The three amigos

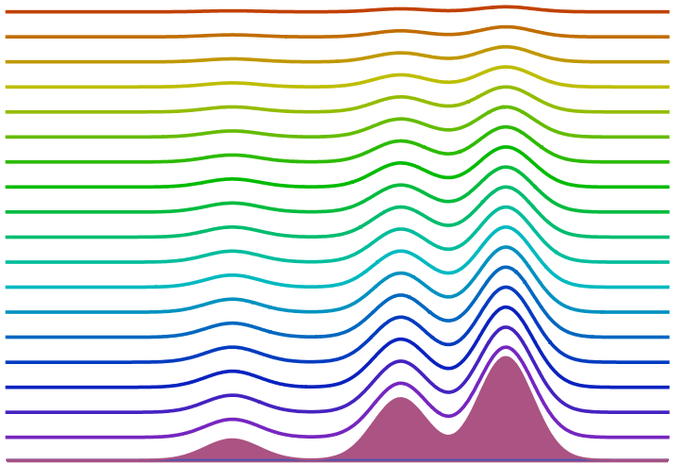

sigma coordinate

Lower boundary is a coordinate surface.

Mass flows freely across layer edges.

Pressure-gradient force is not a gradient.

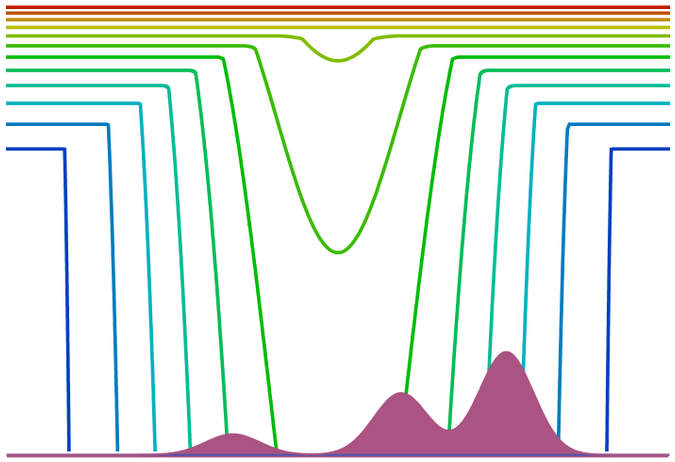

isentropic coordinate

Lower boundary is not a coordinate surface.

Mass flows stays within layers except for heating.

Pressure-gradient force is a gradient.

Massless layers are “lost” in the tropics.

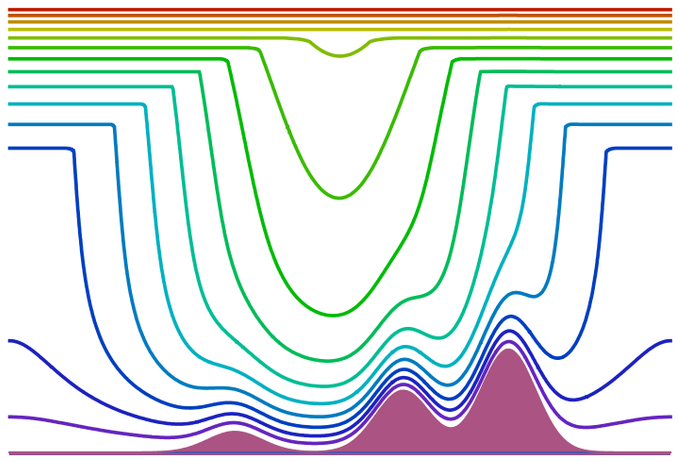

hybrid coordinate

Behaves like sigma near the lower boundary.

Becomes theta smoothly and naturally throughout most of the troposphere and all of the stratosphere.

High-res lower troposphere.

Generalized vertical coordinate

(Konor and Arakawa)

Suppose that ζ is of the form

$$\zeta = f(\sigma) + g(\sigma)\theta$$

where σ increases upward, so that

$$g(\sigma) \to 0 \quad \text{as} \quad \sigma \to \sigma_S$$

$$f(\sigma) \to 0 \quad \text{and} \quad g(\sigma) \to 1 \quad \text{as} \quad \sigma \to \sigma_T$$

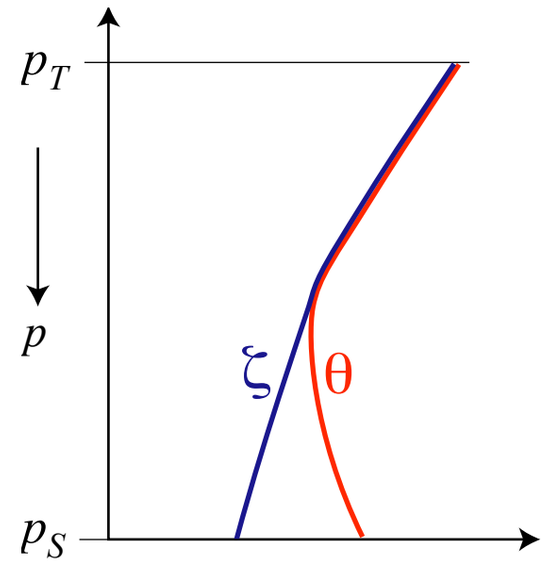

We require monotonicity:

$$\frac{\partial \zeta}{\partial \sigma} = \frac{\partial f}{\partial \sigma} + \frac{\partial g}{\partial \sigma}\theta + g\frac{\partial \theta}{\partial \sigma} > 0$$

which can be ensured by choosing

$$\frac{\partial f}{\partial \sigma} + \frac{\partial g}{\partial \sigma}\theta_{\min} + g\left(\frac{\partial \theta}{\partial \sigma}\right)_{\min} = 0, \quad g > 0, \quad \frac{\partial g}{\partial \sigma} > 0$$

We specify $g(\sigma)$ and solve for $f(\sigma)$.

Example

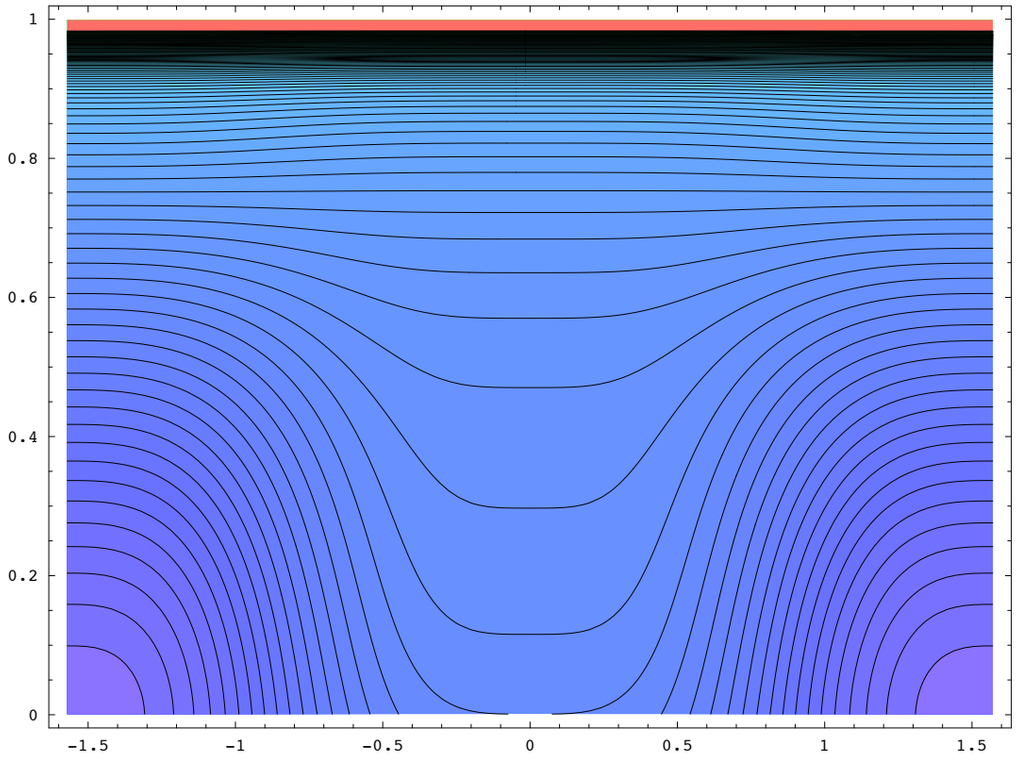

Theta

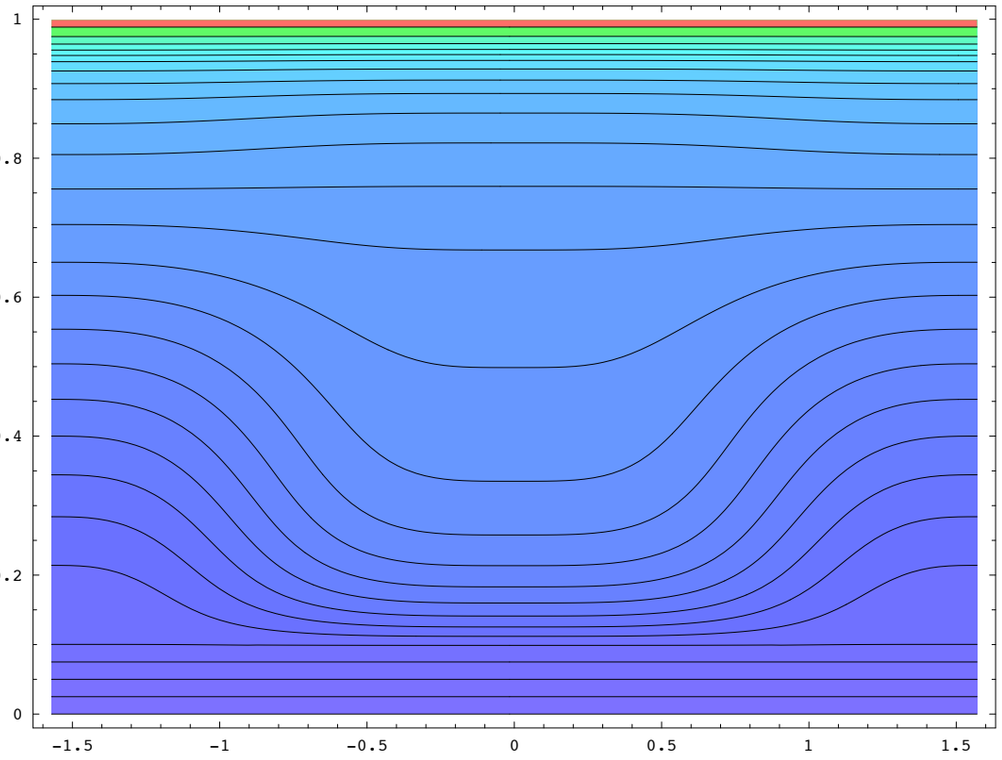

Zeta

Vertical staggering

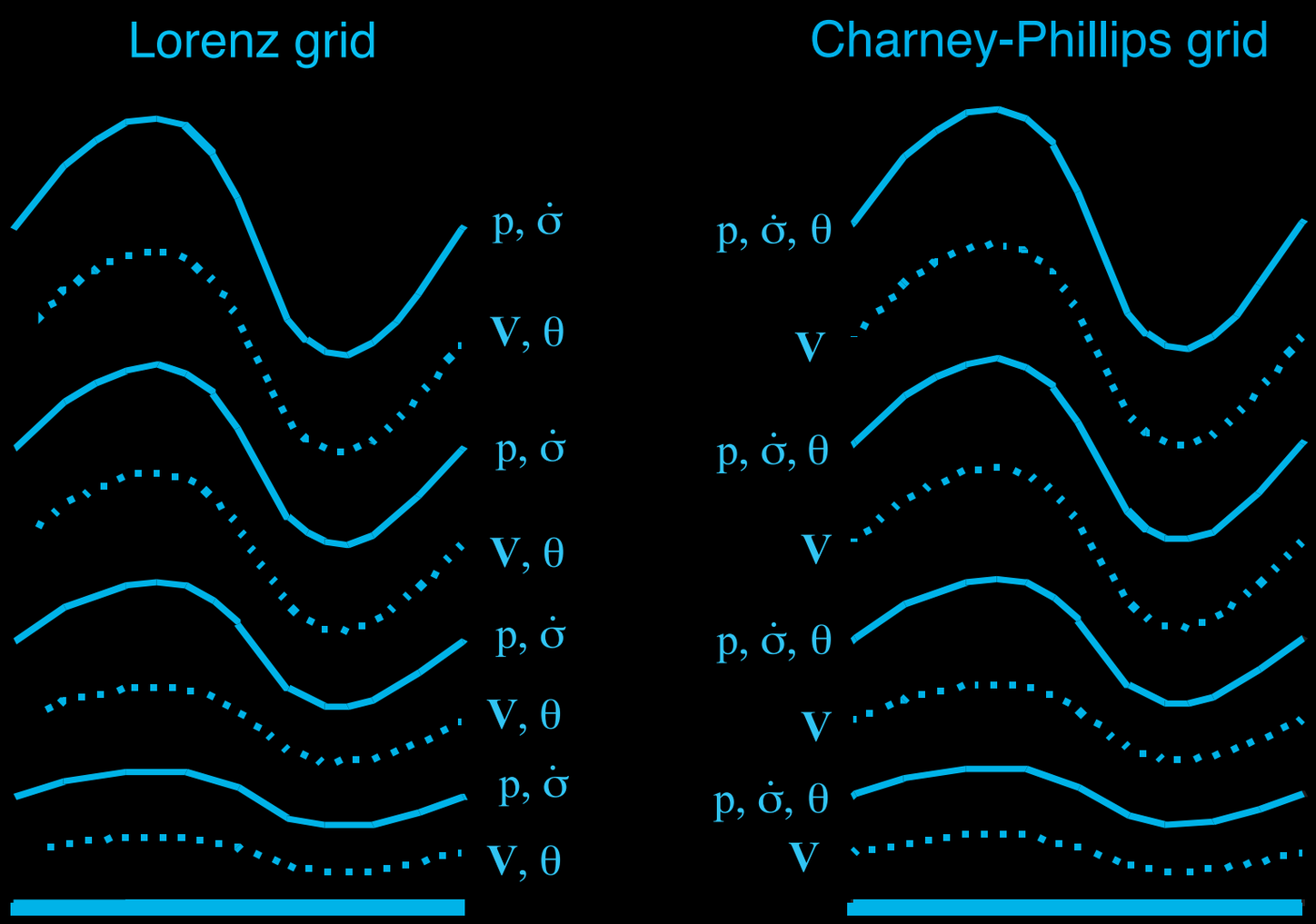

The L-grid has a stationary computational mode in the temperature, while the CP grid does not.

The CP-grid knows about potential vorticity.

Starting HS

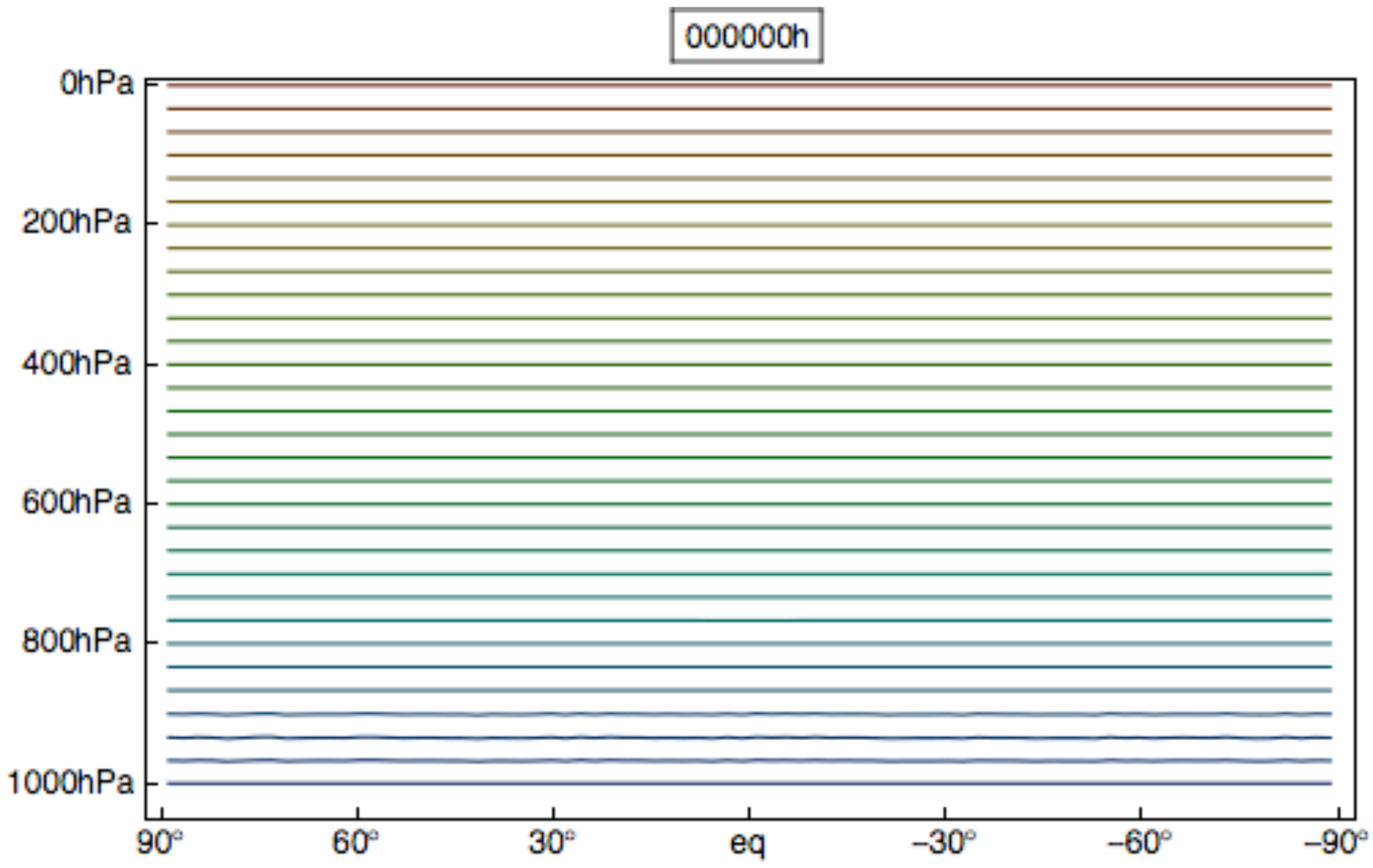
000000h
0hPa
200hPa
400hPa
600hPa
800hPa
1000hPa
90°
60°
30°
eq
−30°
−60°
−90°

The mass streamfunction in sigma coordinates for the zonally averaged mass transport is defined by

$$\frac{\partial \Psi_\sigma}{\partial \varphi} = 2\pi a^2 \cos\varphi \overline{\left[m_\sigma \dot{\sigma} \right]} \quad \text{and} \quad \frac{\partial \Psi_\sigma}{\partial \sigma} = -2\pi a \cos\varphi \overline{\left[m_\sigma v \right]}$$

The Hadley circulations extend from equator to mid-latitudes. The Ferrell circulations are poleward of the Hadley circulations.

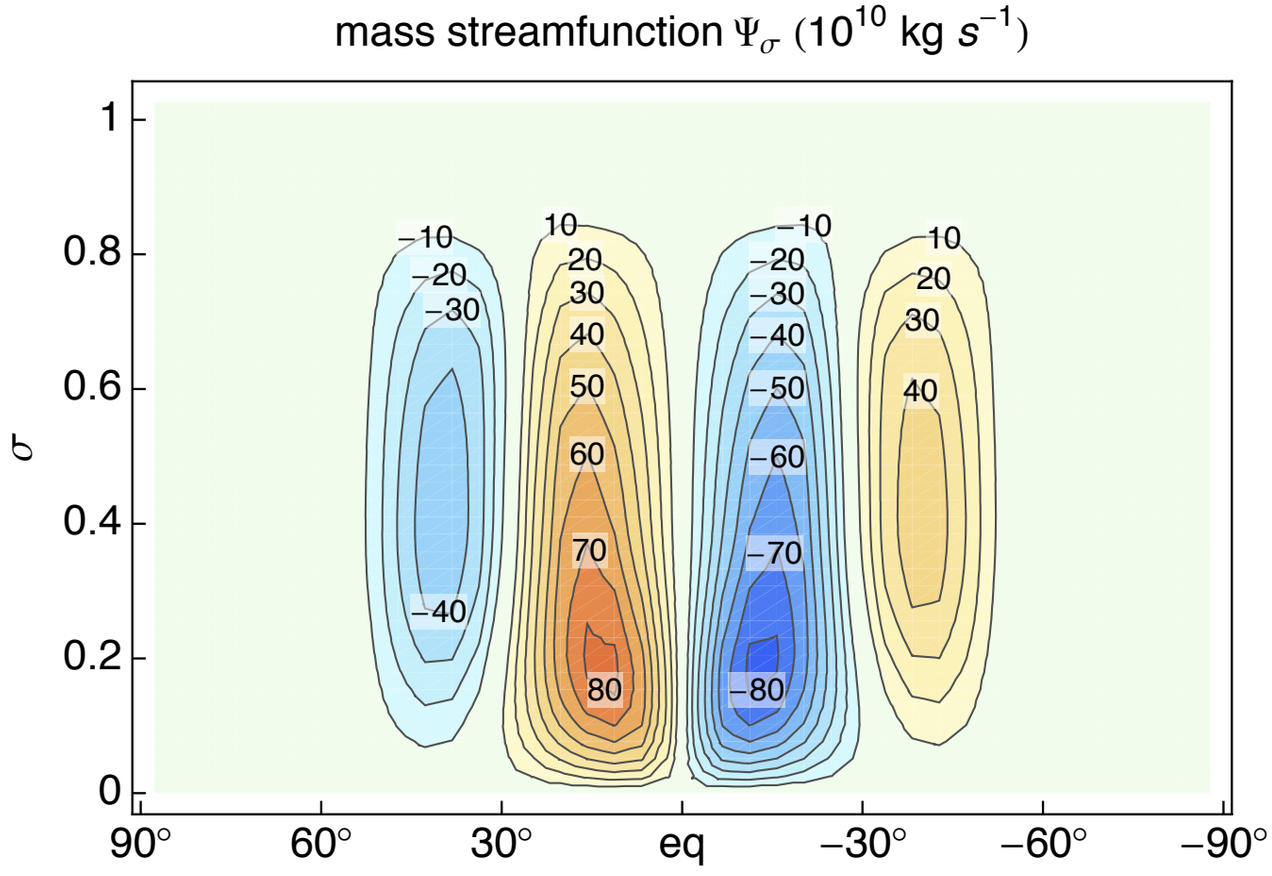

The isentropic mass streamfunction for the zonally averaged mass transport is defined by

$$\frac{\partial \Psi_\theta}{\partial \varphi} = 2\pi a^2 \cos\varphi \overline{\left[m_\theta \dot{\theta} \right]} \quad \text{and} \quad \frac{\partial \Psi_\theta}{\partial \theta} = -2\pi a \cos\varphi \overline{\left[m_\theta v \right]}$$

The Hadley circulations extend from equator to pole. No Ferrell circulations.

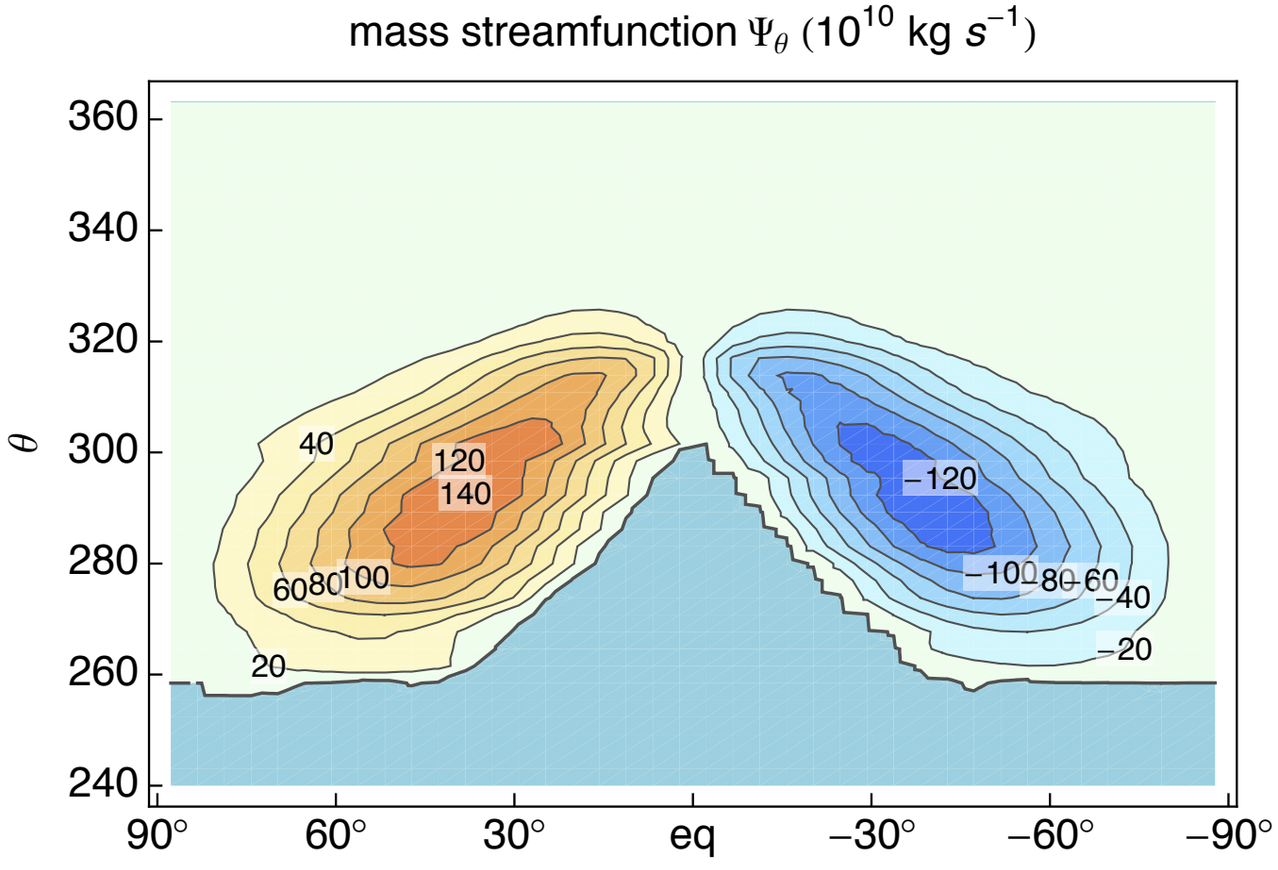

Towsend & Johnson, 1985

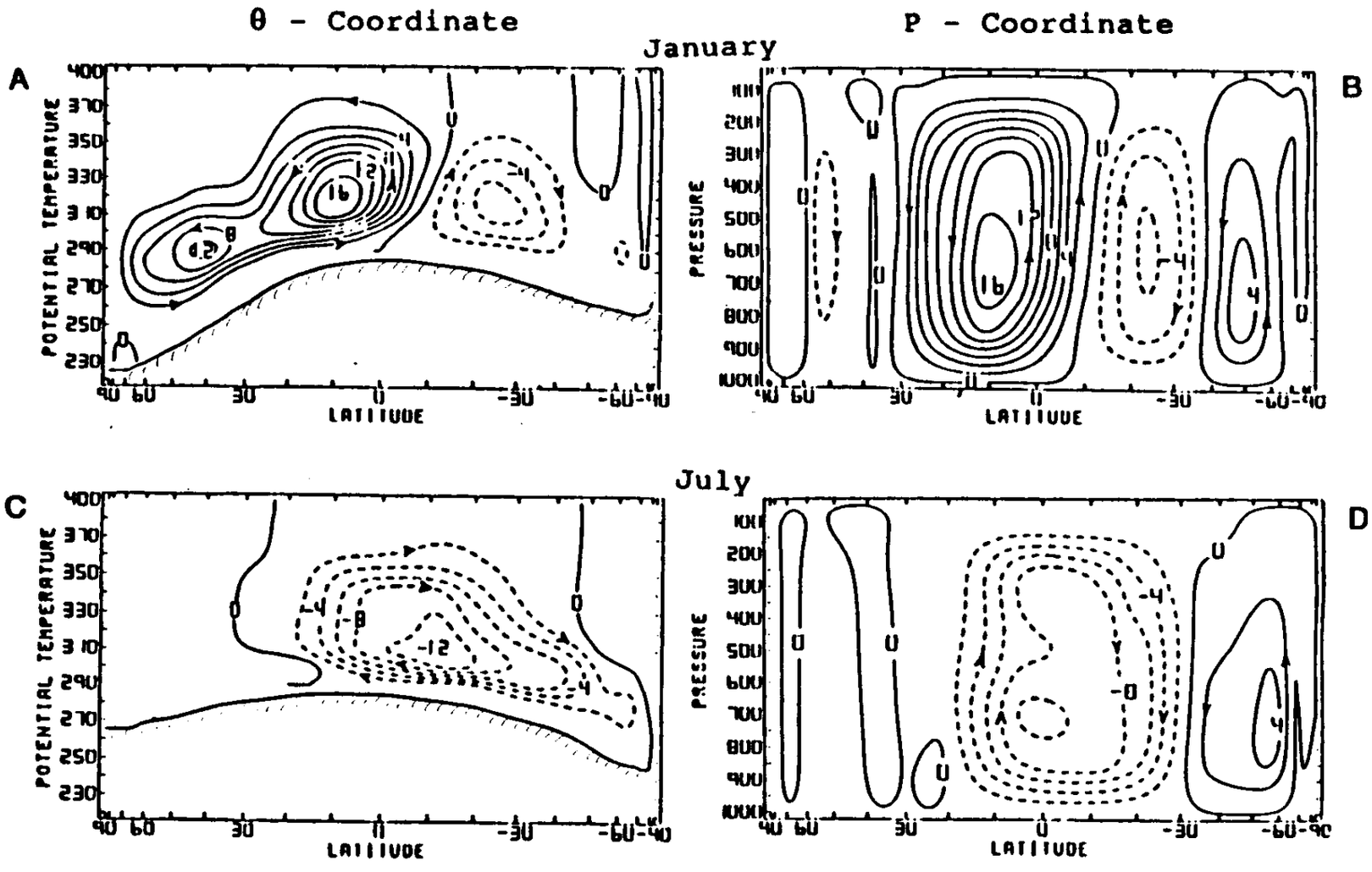

Simulation of a Major Stratospheric Sudden Warming Event and Flow Recovery in the Northern Hemisphere

- **We have tested an isentropic version of the model vertical coordinate model simulating the sudden warming event of February 1979.**

- **Isentropic coordinates are particularly useful for this simulation since diabatic effects are relatively weak.**

- **The geodesic grid avoids the converging meridians at high latitudes. This allows for an isotropic distribution of grid points near the pole.**

Simulation of a Major Stratospheric Sudden Warming Event and Flow Recovery in the Northern Hemisphere

- The observed (NCEP/NCAR) and simulated geopotential height (contour) and temperature (color filled) on the 10 hPa isobaric surface

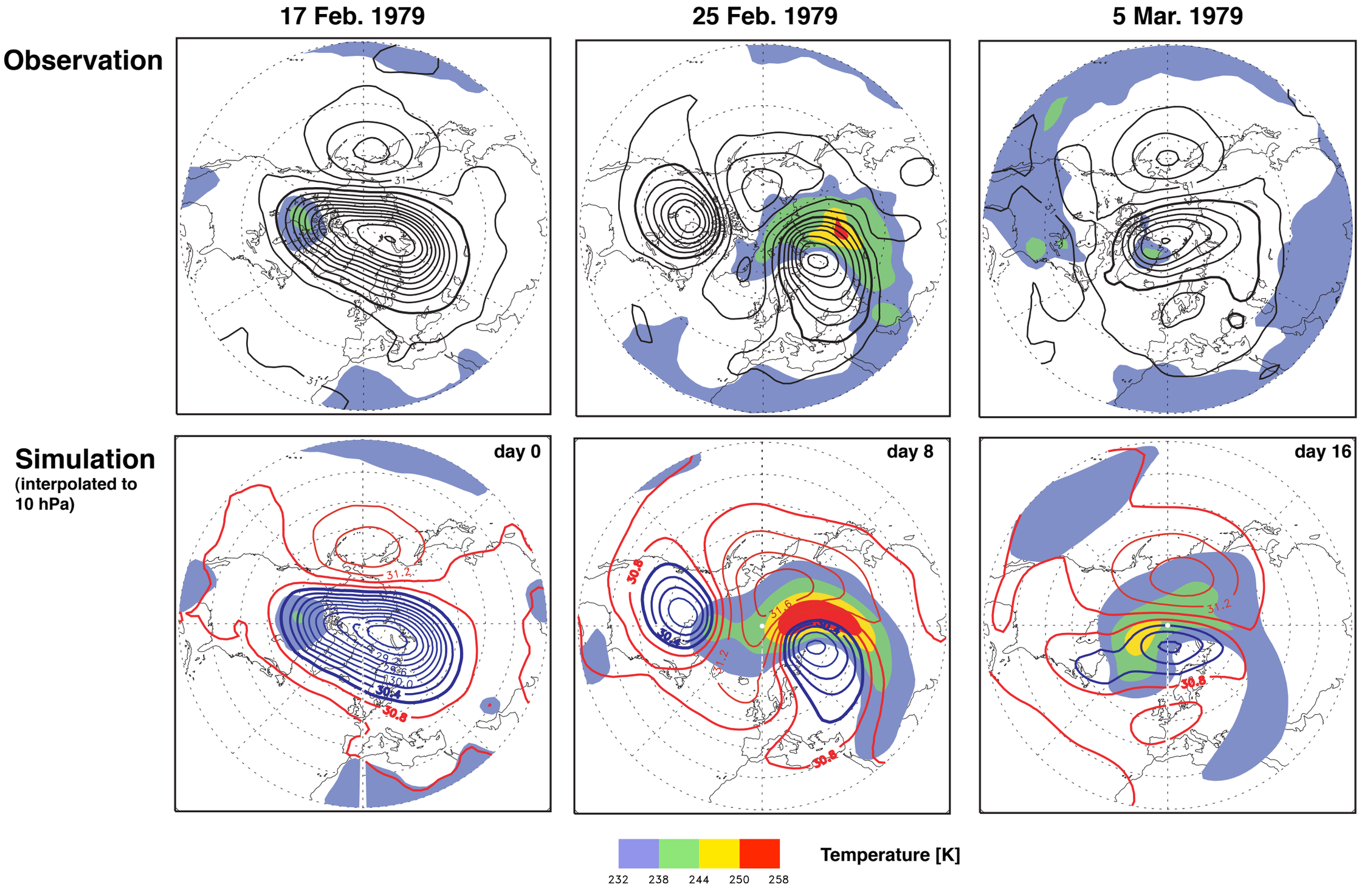

We decided to build a geodesic coupled model.

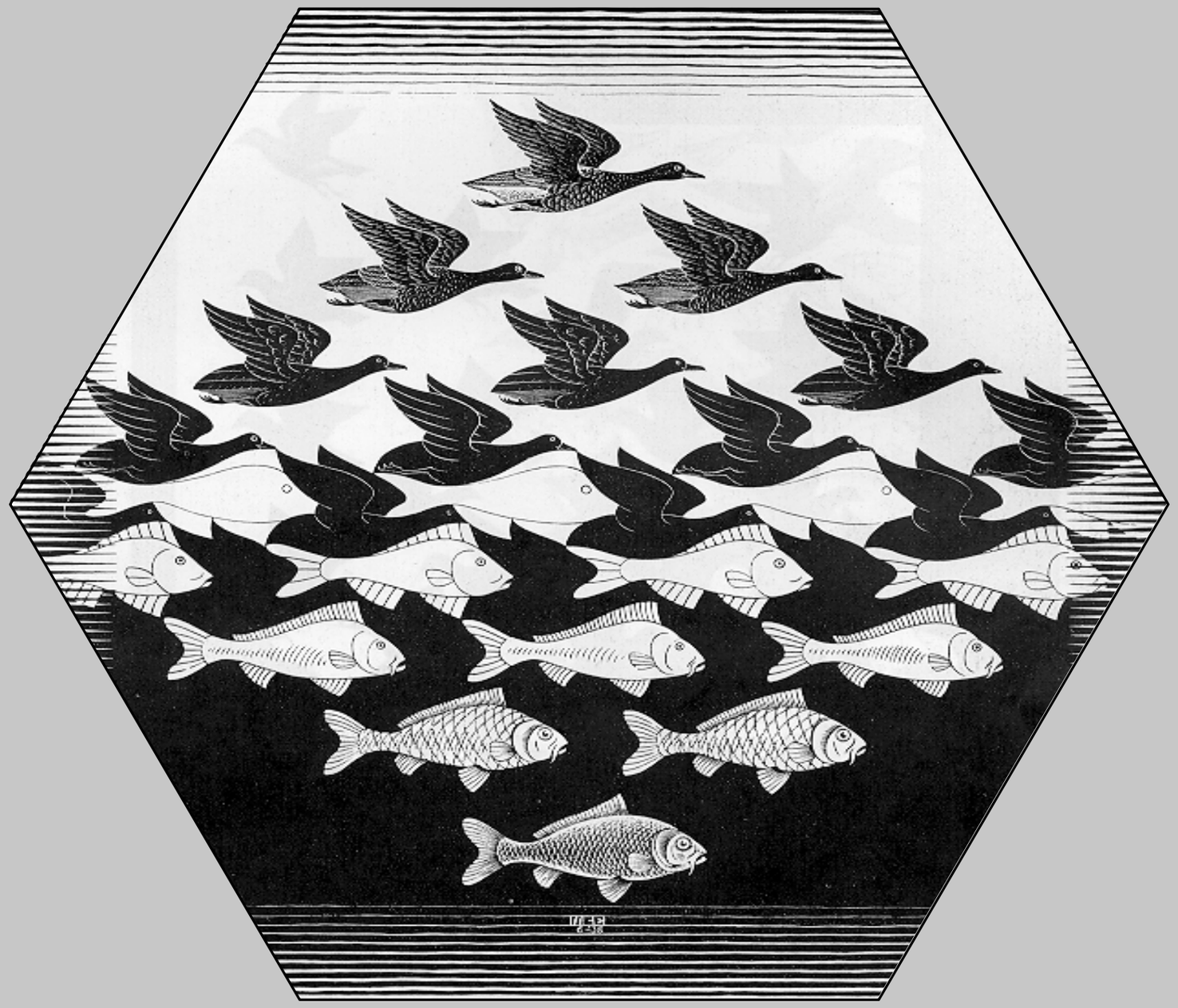

Geodesic Ocean Model

- *First version built by Todd Ringler.*
- *Geodesic ocean shares a lot of code with the geodesic atmosphere.*
- *Ocean physics (initially) based on that of POP.*

Equatorial cross section
10242

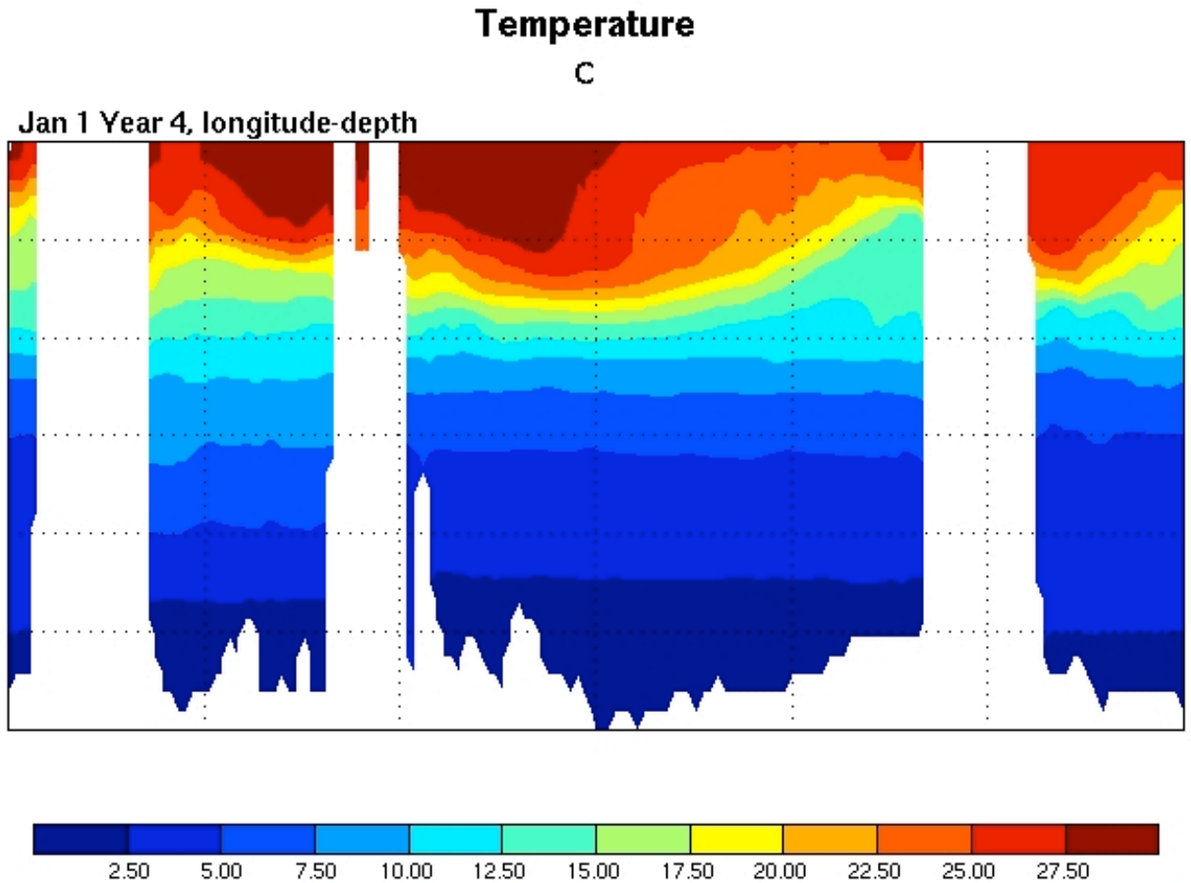

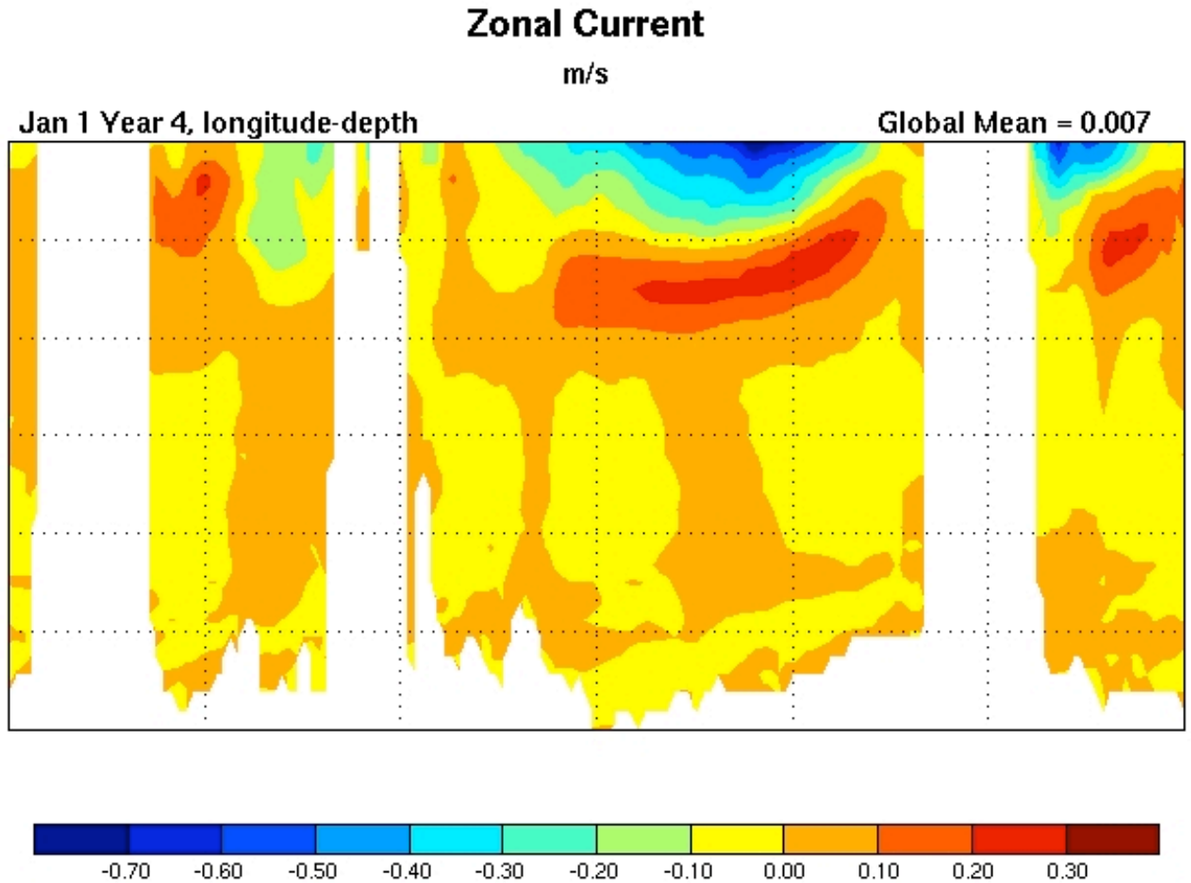

Sea surface height rel to SL

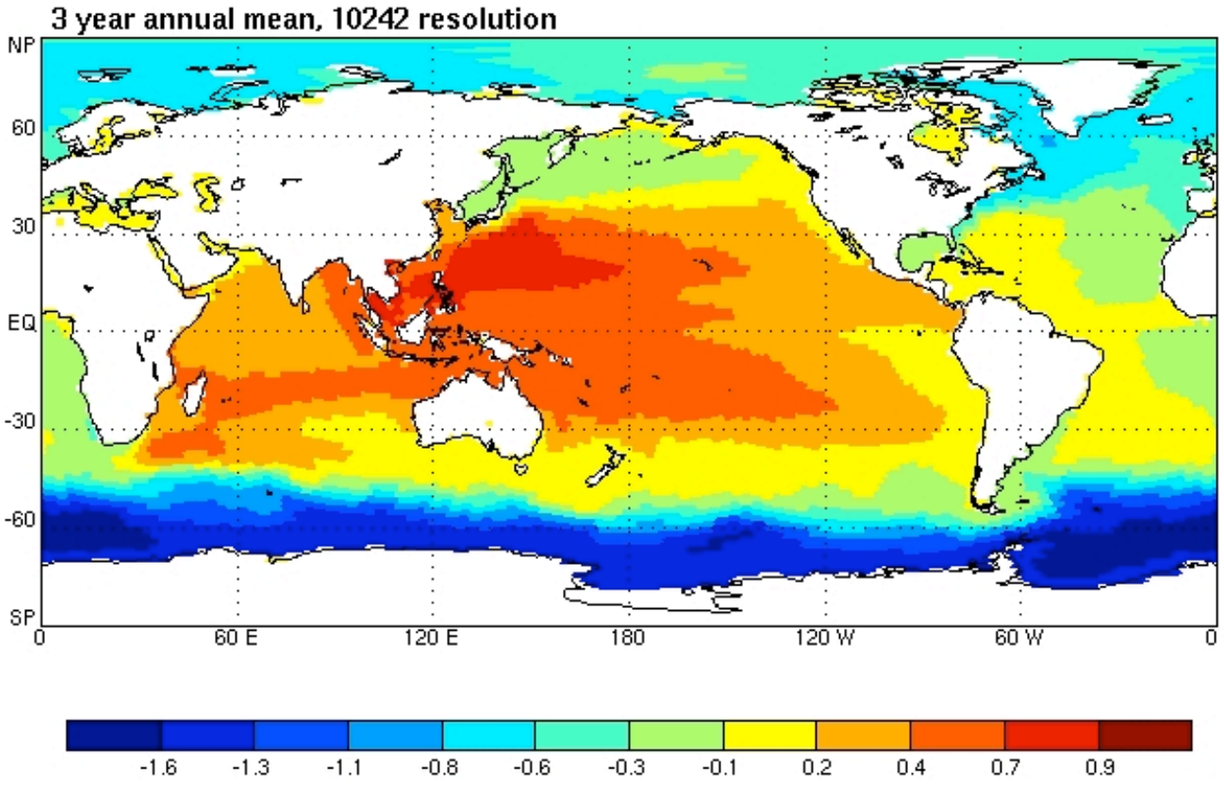

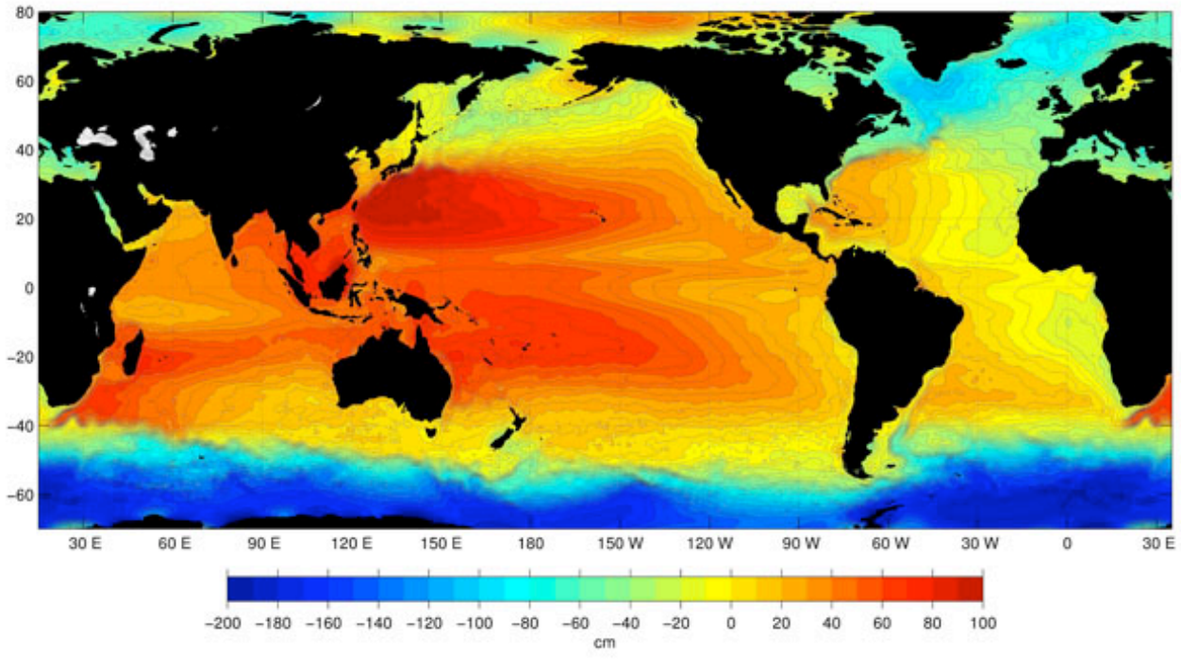

Status

Ocean model is being actively tested and further developed by two researchers at CSU.

Looking to the future...

Non-hydrostatic hybrid-coordinate regional model

- **Mike Toy's disseratation, to be defended in about a month**

- **Tested on Boulder windstorm case -- breaking mountain waves**

- **ALE, but tries to be Konor-Arakawa coordinate**

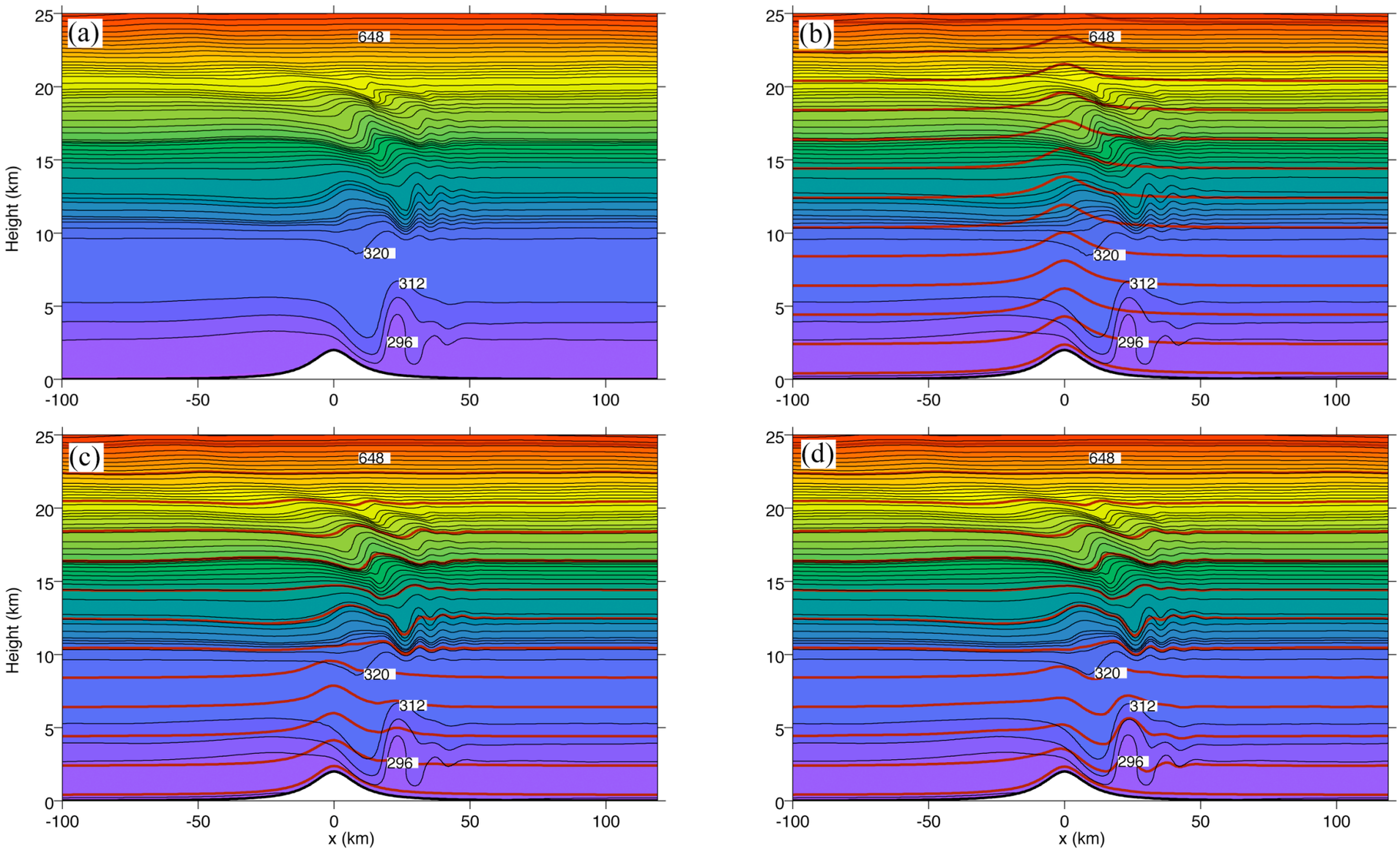

Figure 5.20: Isentropic surfaces (black curves) at time $t = 1\text{hr}10\text{min}$ for the 11 January 1972 Boulder windstorm simulations using the σ coordinate with (a) 500 levels and (b) 125 levels in the lowest 25 km, and the hybrid coordinate with 125 levels in the lowest 25 km for (c) $\theta_{\text{min}} = 20\,\text{K}$ and (d) $\theta_{\text{min}} = 270\,\text{K}$. The contour interval is 8 K and selected isentropes are labeled. The bold red curves in panels (b)-(d) show the locations of every tenth model coordinate surface.

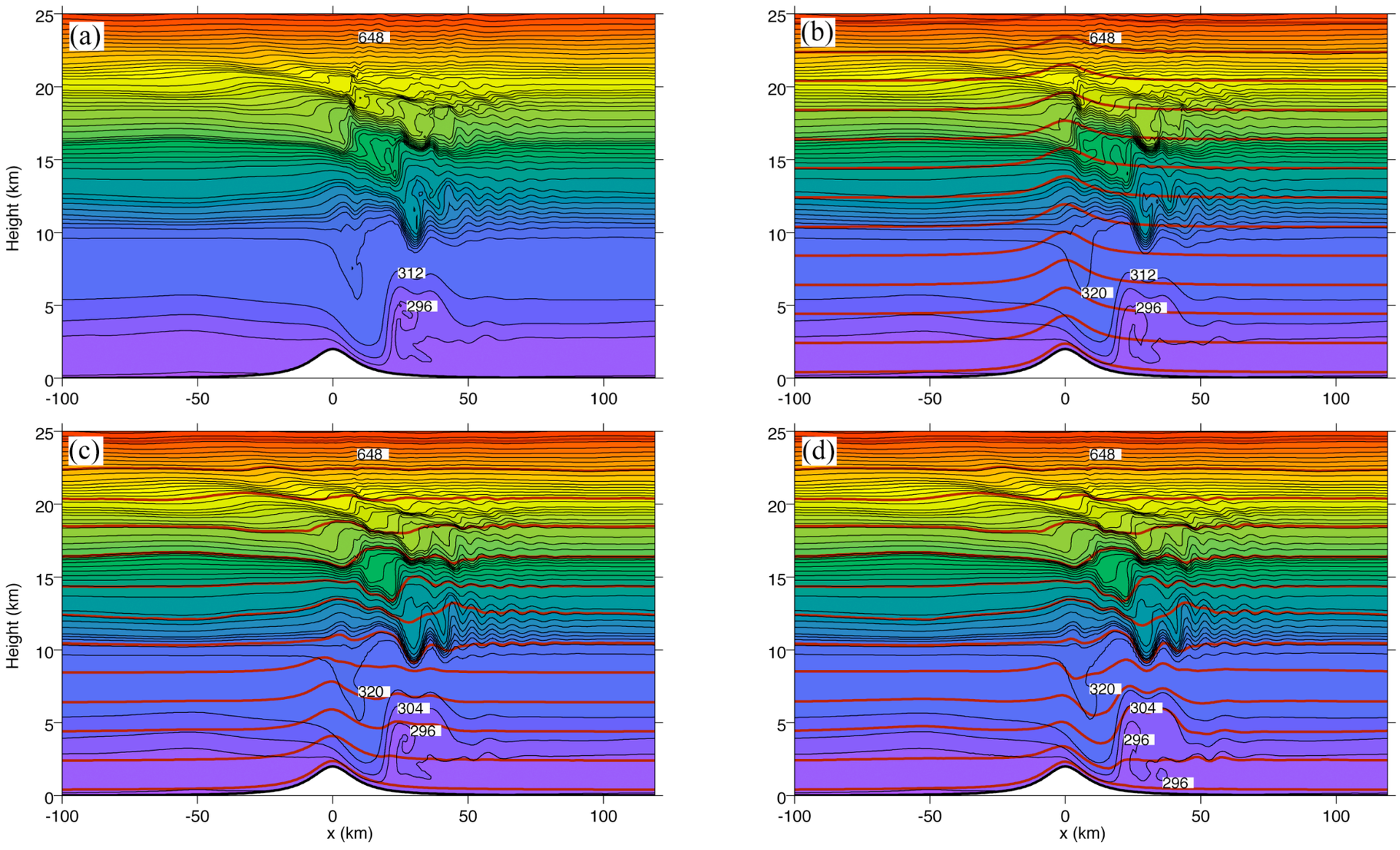

Figure 5.21: Isentropic surfaces (black curves) at time $t = 2$hours for the 11 January 1972 Boulder windstorm simulations using the σ coordinate with (a) 500 levels and (b) 125 levels in the lowest 25km, and the hybrid coordinate with 125 levels in the lowest 25 km for (c) $\theta_{\min} = 20\,\mathrm{K}$ and (d) $\theta_{\min} = 270\,\mathrm{K}$. The contour interval is 8 K and selected isentropes are labeled. The bold red curves in panels (b)-(d) show the locations of every tenth model coordinate surface.

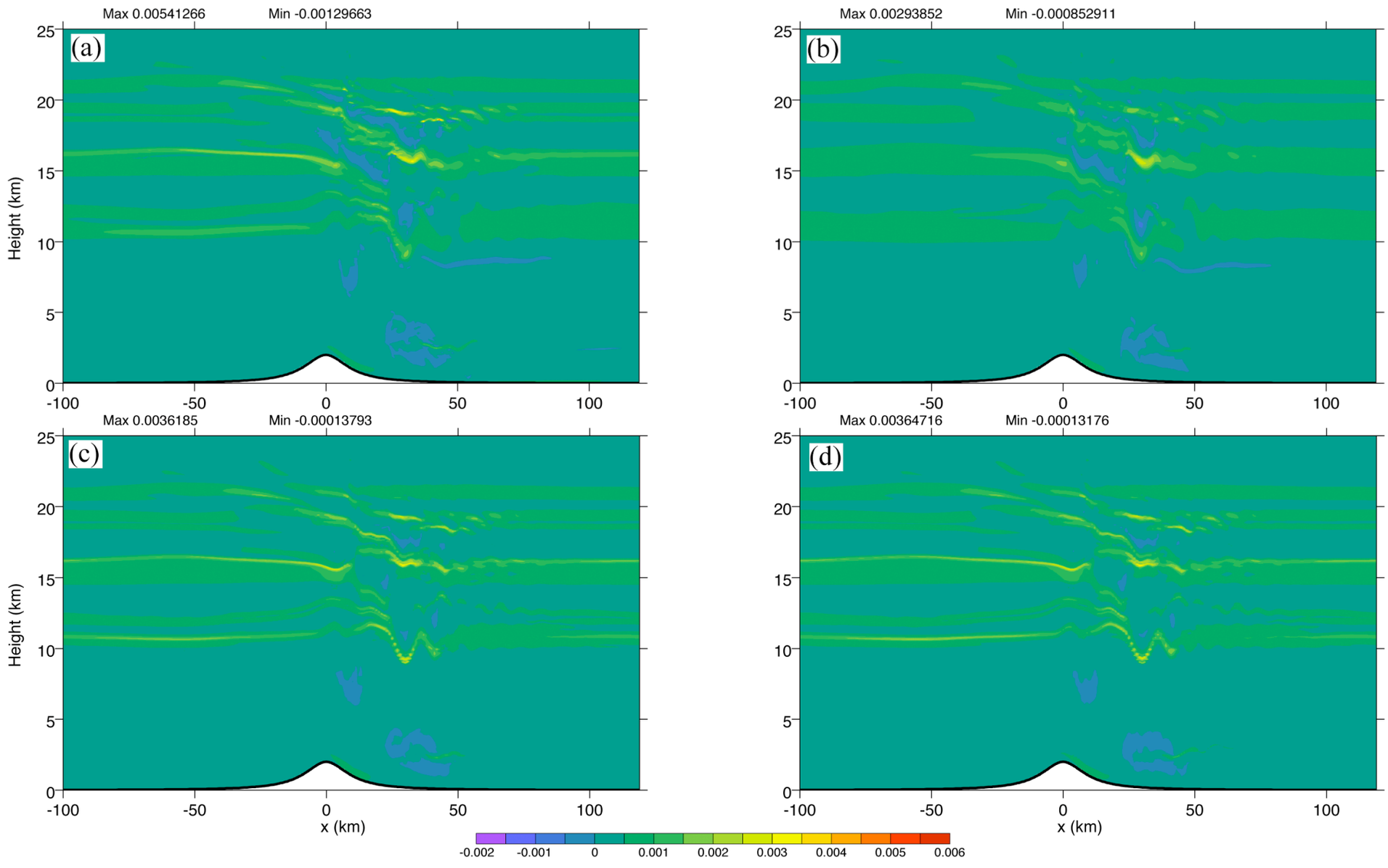

Figure 5.22: Static stability $N^2 = g\theta^{-1}\partial\theta/\partial z$ at time $t = 2$ hours for the 11 January 1972 Boulder windstorm simulations using the σ coordinate with (a) 500 levels and (b) 125 levels in the lowest 25 km, and the hybrid coordinate with 125 levels in the lowest 25 km for (c) $\theta_{min} = 20$ K and (d) $\theta_{min} = 270$ K.

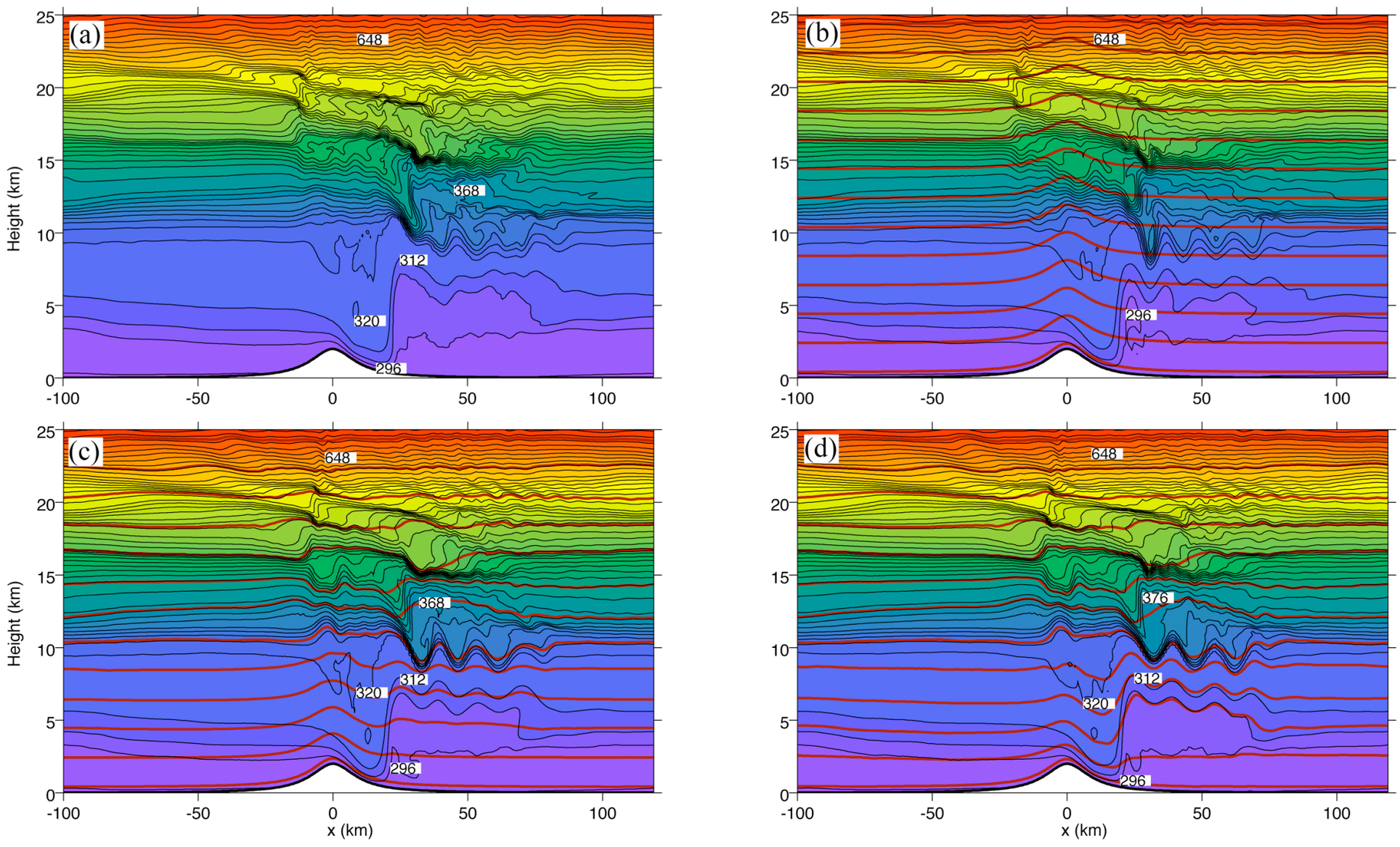

Figure 5.23: Isentropic surfaces (black curves) at time $t = 3$hours for the 11 January 1972 Boulder windstorm simulations using the σ coordinate with (a) 500 levels and (b) 125 levels in the lowest 25km, and the hybrid coordinate with 125 levels in the lowest 25 km for (c) $\theta_{\min} = 20\,\mathrm{K}$ and (d) $\theta_{\min} = 270\,\mathrm{K}$. The contour interval is 8 K and selected isentropes are labeled. The bold red curves in panels (b)-(d) show the locations of every tenth model coordinate surface..

Vector-vorticity cloud model (VVCM)

Upper Boundary

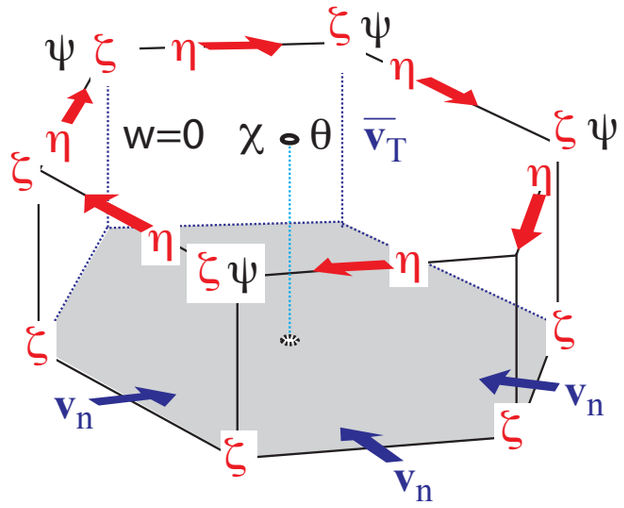

Interior

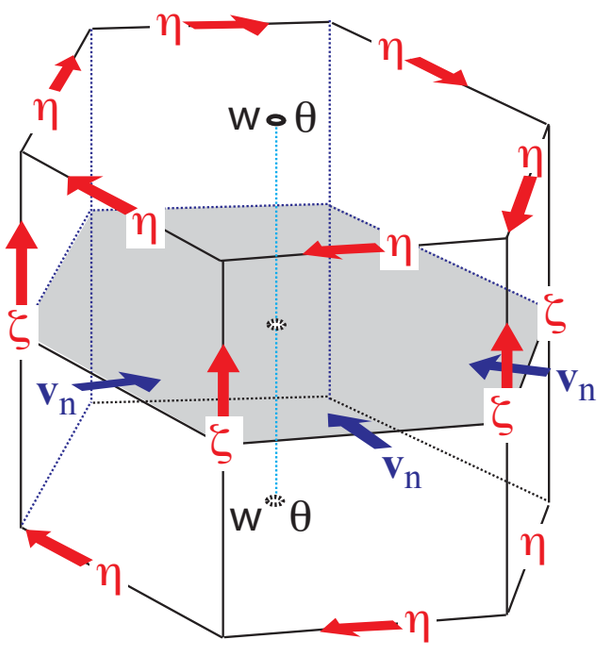

Charney-Phillips Vertical Grid

——— η $\overline{v}_T$ θ ρ_{qs} w=0 ——— z_T

---------- ζ v_n p_{qs} δp --------- z_L

——— η θ w ρ_{qs} ——— $z_{\ell+1/2}$

---------- ζ v_n p_{qs} δp ---------- z_ℓ

——— η θ w ρ_{qs} ——— $z_{\ell-1/2}$

---------- ζ v_n p_{qs} δp ---------- z_1

——— η θ ρ_{qs} w=0 ——— z_S

Multigrid Scaling

Scaling tests were performed on four platforms:

1. **Seaborg at the National Energy Research Scientific Computing Center (NERSC). IBM SP with 6,080 375 MHz POWER 3 processors.**

2. **Blue Gene/L at Argonne. 1024 dual PowerPC 440 700MHz 512MB nodes.**

3. **Jaguar at the National Center for Computational Sciences (NCCS). Cray XT containing a combination of XT3 and XT4 systems. Each node contains 2.6 GHz dual-core AMD Opteron processors and 4 GB of memory.**

4. **Franklin at the National Energy Research Scientific Computing Center (NERSC). Cray XT4 system with 9,660 compute nodes. Each node has dual processor cores, and the entire system has a total of 19,320 processor cores of a 2.6 GHz dual-core AMD Opteron processors. Each compute node has 4 GBytes of memory.**

Multigrid Scaling

The x-axis is number of processes and the y-axis is time.

The blue square indicates grid resolution

The red line is ideal speed-up

Level of recursion	Number of grid columns	Distance between grid columns, km
9	2,621,442	15.64
10	10,485,762	7.819
11	41,943,042	3.909
12	167,772,162	1.955

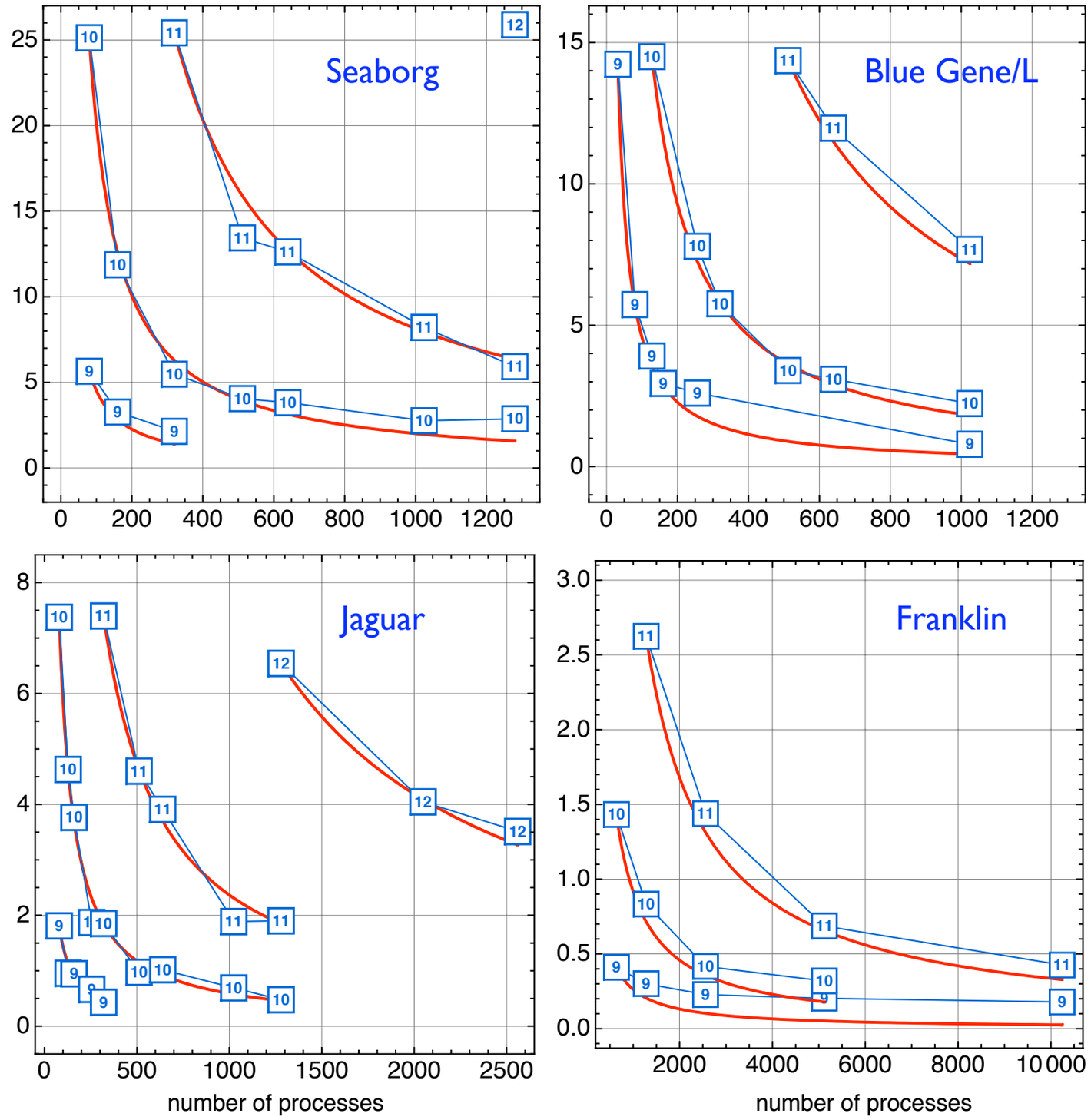

GCRM dynamical core scaling tests

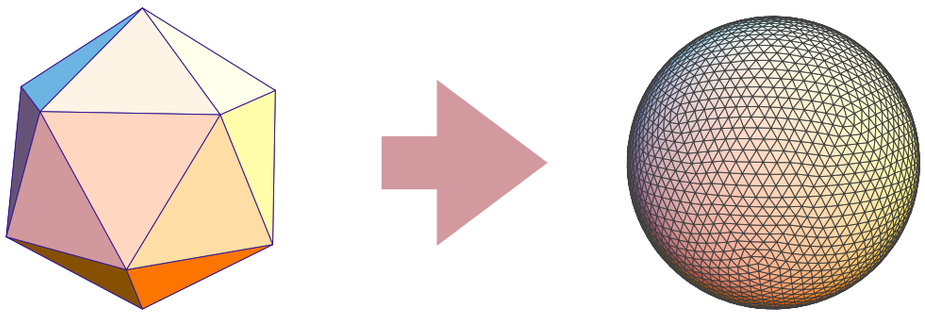

Level of recursion	Number of grid columns	Distance between grid columns, km
9	2,621,442	15.64
10	10,485,762	7.819
11	41,943,042	3.909
12	167,772,162	1.955

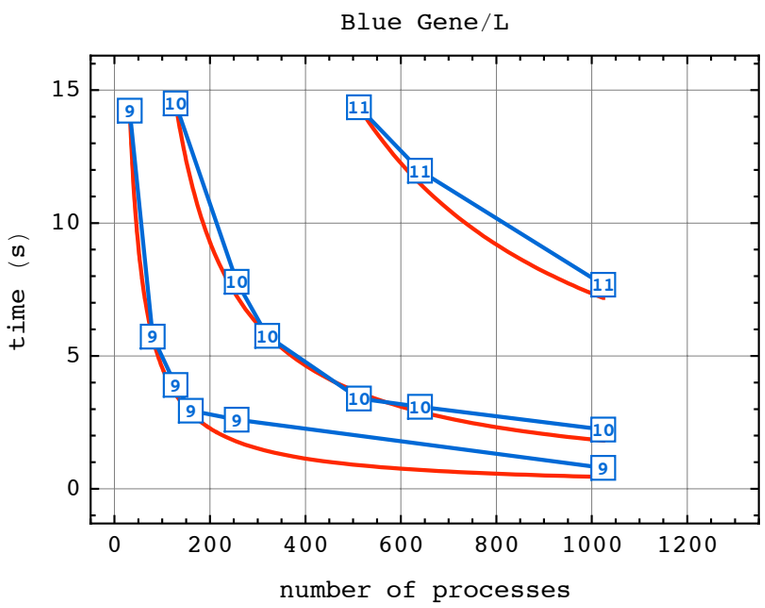

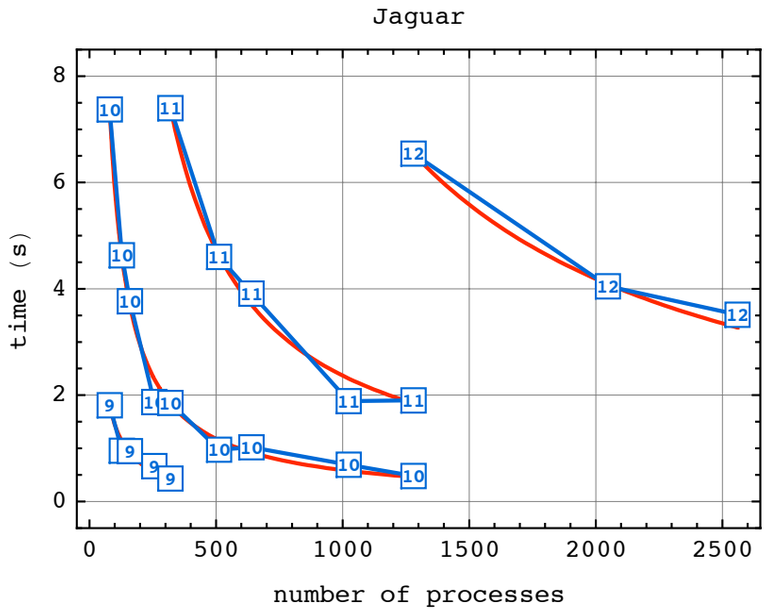

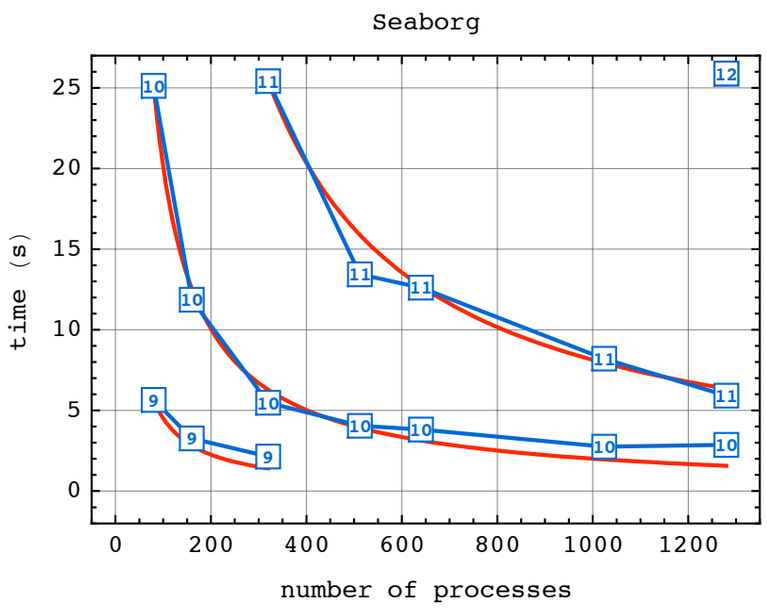

Summary

We have created atmosphere, ocean, sea ice, and land-surface models that use geodesic grids.

The atmosphere model uses a hybrid vertical coordinate.

A regional non-hydrostatic hybrid coordinate model is working now.

A geodesic, non-hydrostatic GCRM is under construction.